

**CO-PRODUCTION OF BIO-BASED FUELS AND CHEMICALS: PROCESS  
MODELING AND ANTICIPATORY LIFECYCLE ENVIRONMENTAL IMPACT  
ASSESSMENT**

by

**Andrew W. Beck**

B.S. Chemical Engineering, University of Pittsburgh, 2015

Submitted to the Graduate Faculty of  
Swanson School of Engineering in partial fulfillment  
of the requirements for the degree of  
Master of Science

University of Pittsburgh

2017

UNIVERSITY OF PITTSBURGH  
SWANSON SCHOOL OF ENGINEERING

This thesis was presented

by

Andrew W. Beck

It was defended on

November 28, 2017

and approved by

Melissa M. Bilec, PhD, Associate Professor, Civil and Environmental Engineering Department

Carla A. Ng, PhD, Assistant Professor, Civil and Environmental Engineering Department

Thesis Advisor: Vikas Khanna, PhD, Associate Professor, Civil and Environmental Engineering

Department

Copyright © by Andrew W. Beck

2017

**CO-PRODUCTION OF BIO-BASED FUELS AND CHEMICALS: PROCESS MODELING  
AND ANTICIPATORY LIFECYCLE ENVIRONMENTAL IMPACT ASSESSMENT**

Andrew W. Beck, M.S.

University of Pittsburgh, 2017

Heralded as a technology to address anthropogenic climate change, resource renewability, and national energy security, biofuels and their many production pathways have continued to scale up and develop globally. While economic feasibility is always explicitly considered in designing biorefineries and supply chains, environmental performance is often evaluated retrospectively or assumed to improve on baseline petroleum fuels. As such, many early biofuel technologies resulted in unexpected environmental consequences, prompting researchers to propose systematic frameworks to conduct forward-looking “anticipatory” lifecycle assessments (LCA), to quantify environmental impacts during the design phase of biofuel production pathways. Such analyses have gained further utility as countries implement low-carbon fuel tax credits, requiring companies to quantify lifecycle greenhouse gas (GHG) emissions for biofuels and demonstrate reductions versus a similar petroleum fuel. Allowing for further improvements in environmental performance, specialty and commodity organic chemicals can also be derived from biomass feedstocks in tandem with fuel production. In light of these considerations, this work evaluates the environmental performance of an array of biorefinery designs that co-produce bio-based fuels and chemicals. Chemical process models and a prospective well-to-wheel LCA model of a two-step multistage torrefaction and catalytic upgrading system are constructed to quantify lifecycle GHG emissions and energy return on primary fossil energy investment ( $EROI_{\text{fossil}}$ ) for a drop-in replacement biofuel product. Cyclopentanone, biochar, and a net electricity export are each generated as potential co-products,

and assessed under market-based allocation and displacement methods. Across design cases, process performance metrics and LCA results are compared to evaluate trade-offs between process and environmental performance. LCA results are generated with measures of uncertainty, and undergo sensitivity analyses to identify the most influential model parameters. Modeling results suggest that insofar as markets allow, removing bio-chemicals upstream can reduce hydrogen consumption, utilities consumption, and equipment sizing without excessive loss in fuel production – an integral step towards commercially feasible biorefineries. Finally, methodological limitations of accounting schemes for both GHG and  $EROI_{fossil}$  are explored and discussed due to the distortions they produce under the co-production of fuels and chemicals. While GHG emissions may be better addressed via consequential LCA, co-product crediting within EROI requires a full mathematical overhaul.

## TABLE OF CONTENTS

<b>ACKNOWLEDGEMENTS .....</b>	<b>XIII</b>
<b>1.0 INTRODUCTION.....</b>	<b>1</b>
<b>2.0 PROCESS DESIGN AND MODELING.....</b>	<b>11</b>
<b>2.1 PROCESS DESCRIPTION .....</b>	<b>11</b>
<b>2.2 UPGRADING CHEMISTRIES .....</b>	<b>14</b>
<b>2.3 CHEMICAL PROCESS MODELING.....</b>	<b>19</b>
<b>3.0 LIFECYCLE ASSESSMENT STUDY DESIGN .....</b>	<b>26</b>
<b>3.1 LIFECYCLE GOAL AND SCOPE .....</b>	<b>26</b>
<b>3.2 LIFECYCLE INVENTORY, IMPACT MODELING, AND CO-PRODUCT HANDLING .....</b>	<b>27</b>
<b>3.3 LIFECYCLE IMPACT METRICS .....</b>	<b>30</b>
<b>3.4 UNCERTAINTY AND SENSITIVITY ANALYSIS.....</b>	<b>31</b>
<b>4.0 RESULTS AND DISCUSSION .....</b>	<b>33</b>
<b>4.1 PRODUCT DISTRIBUTION.....</b>	<b>33</b>
<b>4.2 PROCESS CARBON FLOWS.....</b>	<b>34</b>
<b>4.3 PROCESS-SCALE METRICS.....</b>	<b>36</b>
<b>4.4 LIFECYCLE GHG EMISSIONS AND EROI.....</b>	<b>37</b>
<b>4.5 SENSITIVITY ANALYSIS .....</b>	<b>47</b>

<b>5.0</b>	<b>CONCLUSIONS AND FUTURE WORK .....</b>	<b>50</b>
<b>5.1</b>	<b>METHODOLOGICAL LIMITATIONS.....</b>	<b>50</b>
<b>5.2</b>	<b>FUTURE WORK.....</b>	<b>52</b>
	<b>BIBLIOGRAPHY .....</b>	<b>54</b>

## LIST OF TABLES

Table 1. Yield values given as weight percentages of ash-free biomass input, for a bench-scale multistage torrefaction and pyrolysis system, representing bio-oil constituents via a set of seven model compounds.....	12
Table 2. Total process utility requirements for all CPO co-production scenarios, including electricity and heat demands from pressure and temperature conditioning unit operations. Minimum heating and cooling duties are calculated via pinch analysis, and electricity values are acquired from Aspen v10 simulation results .....	24
Table 3. Lifecycle unit process and impact factor data sources, also including confidence interval information and sample size <i>N</i> accessed (if available).....	28
Table 4. Summary of LCI statistical metadata, including distribution types and parameter values. Statistical information for direct land use change, cuttings production, and woody biomass production modules are derived from and presented in Zaimes et. al, 2017 .....	31
Table 5. Yield- and efficiency-oriented process performance metrics for each co-production scenario .....	37
Table 6. Median values for lifecycle GHG emissions (gCO <sub>2</sub> e/MJ-Fuel) for all design cases, given in the form X (Y,Z) where X = 50th percentile, Y = 10th percentile, and Z = 90th percentile.....	39

Table 7. Median values for  $EROI_{fossil}$  (MJ-Fuel/MJ-Primary Fossil Energy) for all design cases, given in the form X (Y,Z) where X = 50th percentile, Y = 10th percentile, and Z = 90th percentile..... 39

Table 8. Primary product (biofuel) and co-product shares of total mass and revenue outputs..... 50

## LIST OF FIGURES

Figure 1. Process flow diagram containing SRWC agricultural modules, pre-treatment processing steps, and the full sets of thermal decomposition and catalytic upgrading unit operations in the biorefinery model. Heat and electricity flows from the combined heat and power (CHP) unit are consumed within the system boundary according to utility demands; only excess electricity is exported as a co-product.....	14
Figure 2. Torrefaction bio-oil yield distribution of model compound families.....	15
Figure 3. Aspen process simulation layout for Max Fuel Scenario.....	19
Figure 4. Aspen process simulation layout for Max CPO Scenario.....	20
Figure 5. Aspen process simulation layout for Market CPO Scenario.....	20
Figure 6. Temperature versus enthalpy pinch analysis plots, depicting hot (red) and cold (blue) composite curves for the Max CPO co-production case.....	21
Figure 7. Temperature versus enthalpy pinch analysis plots, depicting hot (red) and cold (blue) composite curves for the Market CPO co-production case.....	22
Figure 8. Temperature versus enthalpy pinch analysis plots, depicting hot (red) and cold (blue) composite curves for the Max Fuel co-production case.....	22
Figure 9. Vapor pressure versus temperature curves for compounds entering the first CPO-separating distillation column, used to assign light and heavy column keys. Toluene	

(grey) is taken as the light key, and cyclopentanone (magenta, hollow del symbol) as the heavy key .....	25
Figure 10. Product carbon distributions of fuel and CPO products (kg C / hr) in Max Fuel, Market CPO, and Max CPO scenarios. Lighter bars indicate quantities of CPO production, and darker bars indicate fuel. Compounds beyond C15 are not produced by any system.....	34
Figure 11.. Process-level carbon flows (kg C / hr) for the Market CPO co-production scenario	35
Figure 12. Box plots of lifecycle GHG emissions and $EROI_{fossil}$ percentile values across all co-product scenarios. As per the above legend, boxes center on median values, and error bars represent the 10 <sup>th</sup> -30 <sup>th</sup> and 70 <sup>th</sup> -90 <sup>th</sup> percentile ranges. The RFS2 GHG reduction threshold for diesel is calculated as 50% of 91.94 g CO <sub>2e</sub> /MJ-diesel .....	38
Figure 13. Contributions of key process inputs and co-product outputs – including CPO – to lifecycle GHG emissions for all co-production and co-product scenarios under the displacement method. ....	42
Figure 14. Contributions of key process inputs and co-product outputs – including CPO – to lifecycle GHG emissions for all co-production and co-product scenarios under the displacement method. ....	43
Figure 15. Contributions of key process inputs and co-product outputs – excluding CPO – to lifecycle primary fossil energy consumption for all co-production and co-product scenarios under the displacement method.....	44
Figure 16. Contributions of key process inputs and co-product outputs – including CPO – to lifecycle primary fossil energy consumption for all co-production and co-product scenarios under the displacement method.....	45

Figure 17. Sensitivity results for 8 model parameters for the Market CPO production case, evaluated under market allocation by varying parameters  $\pm 20\%$  ..... 48

Figure 18. Sensitivity results for 8 model parameters for the Market CPO production case, evaluated under market allocation by varying parameters  $\pm 20\%$ . Fuel Price and CPO price do not affect the LCIA metrics, as would be expected for displacement. Reducing Biochar Yield's affects  $EROI_{fossil}$  in such a way as to shift the metric's denominator from a negative value to a positive value, producing the distorted result shown here ..... 49

## ACKNOWLEDGEMENTS

Thanks are in order to celebrate the many people that kept me sane and afloat throughout this whole process. I owe a deep debt of gratitude to my dear friends Camille, Rachel, Reid, Simon, and Thomas, as they did an especially noteworthy job of this, even as we all continued to spread across the continent. Furthermore, I can't see myself being anywhere near where I am today without the years of unyielding love, support, and guidance from my family.

My primary mentors, Dr. Greg Zaines and Dr. Vikas Khanna, both served as invaluable teachers, sounding boards for nuanced discussion, and continual sources of motivation. For all their support and segments of guiding wisdom, I would like to thank the members of my thesis committee – Drs. Melissa Bilec, Carla Ng, and Vikas Khanna. I also would like to acknowledge the U.S. Department of Energy (DOE) for financially supporting this research.

Lastly, shout out to my various house plants, for (mostly) not dying on me, and for reminding me that growth doesn't happen overnight.

## 1.0 INTRODUCTION

The looming risk of irreversible, runaway climate change continues to grow via anthropogenic emission of greenhouse gases (GHGs) [1]; with respect to energy-related GHG emissions, the transportation sector globally accounted for some 23% of total energy-related emissions in 2010 and 27% in 2015 [2, 3]. As such, many governments have accelerated research activities around and instituted GHG reduction incentives for low-carbon renewable biofuels, including the EU 2008 Fuel Quality Directive [4], the U.S. Environmental Protection Agency's (EPA) updated Renewable Fuels Standard (RFS2) [5], and California's 2007 Low Carbon Fuel Standard [6]. Serving as a drop-in substitute fuel for existing vehicle fleets, low-carbon renewable biofuels can potentially serve to mitigate the increasing contribution of the transportation sector to global GHG emissions, while simultaneously offering nations the ability to increase their domestic energy security [7]. Given the importance of the transition away from fossil energy sources and their associated emissions, biofuel technologies have consistently garnered attention in both public and private spheres, with research and development being simultaneously carried out in both academia and industry. Governments in many countries have continued to explore, regulate, and incentivize their production, in efforts to establish secure sources of energy, provide jobs and economic stimuli to various populations, and cooperatively address climate change within the international community.

In attempts to initiate and then expedite the transition to low-carbon, renewable energy sources, the vast majority of countries in the world have signed international agreements, such as the 1992 Kyoto Protocol derived from the United Nations Framework Convention on Climate Change and the 2015 Paris Climate Accord, to meet carbon reduction goals of various forms [8, 9]. Policies at the nation-scale have varied from carbon taxes to cap-and-trade programs, and also include an ever-growing cornucopia of sector-specific agreements and incentives. For transportation fuels in particular, volumetric production mandates for renewable fuels have emerged both in the U.S. and the EU – the Energy Independence and Security Act of 2007 (EISA) and Renewable Energy Directive (RED) respectively [7, 10]. Within each of these rafts of policies, a host of sourcing requirements and financial incentives have been implemented to reduce the lifecycle carbon intensity of renewable biofuel products below some threshold values, typically established as a percentage reduction versus a substitutable fossil fuel [11]. In particular, the EISA set the mandated U.S. national biofuel production target to increase from 4.7 billion to 36 billion gallons over the years 2007-2022, at the end of which some 21 billion gallons must be derived from non-cornstarch feedstocks, including sugar crops, lipid-producing legumes and grains, and/or cellulosic biomass [7]. This latter requirement also houses the revised RFS2 guidelines from 2010, that require various types of biofuels to meet a corresponding GHG reduction threshold – ranging by category from 50-60% versus baseline petroleum fuels, evaluated using LCA – in order to be categorically considered under within the framework of the policy and acquire a production tax credit [5].

Having learned from mistakes of the past, the aforementioned EISA production mandates explicitly promote increasing production levels of second-generation biofuels over their first-generation predecessors. First generation biofuels are typically divided into two broad categories:

bioethanol, which is derived primarily from the fermentation of sugars and starches from corn, sugarcane, and grains; and biodiesel, produced via transesterification of lipids derived from legumes, seeds, and waste vegetable oil. These feedstocks all directly compete with food crops for use of agricultural land, which some argue may consequently affect the global prices of food [12]. Furthermore, first generation biofuels are not currently economically feasible without subsidies [13], are of nebulous energetic viability [14], and have been characterized as carrying their own set of environmental burdens. Potential impacts include water quality impacts, biodiversity loss, soil erosion/depletion, land-use change impacts [15] – the last of which includes enough uncertainty to potentially nullify the purported GHG benefits of first generation fuels over a petroleum baseline [16, 17]. The full diversity and magnitude of these impacts are particularly troubling in light of their intersection with the works of Rockstrom et. al and Steffen et. al, which assert that humankind have already surpassed certain “planetary boundaries” with respect to land-use and fertilizer run-off into waterways [18, 19].

Second generation feedstocks, such perennial grasses, lignocellulosic short rotation woody crops (SRWCs), microalgae, oil-seeds, and municipal solid waste, have been selected to avoid competition with food crops for agricultural land, and are typically also screened to avoid the environmental shortcomings of the previous generation. Feedstock treatment pathways to produce second generation or “advanced” biofuels include bio-chemical decomposition via microbial and/or enzymatic activity, and thermochemical decompositions such as gasification, pyrolysis, and torrefaction. Pyrolysis and torrefaction in particular have recently received substantial research attention, due to their ability to produce bio-oil streams able to be upgraded into infrastructure-compatible hydrocarbon fuels [20-23]. Pyrolysis is typically carried out between 450-600°C as an anaerobic thermal decomposition of cellulose and hemicellulose, and

produces an array of hydrocarbon vapors, solid biochar, and a host of non-condensable gases (NCGs). Said vapors can be upgraded to transportation-range fuels via well-established petroleum refining and hydroprocessing technologies, or through a more chemically tailored thermochemical upgrading route [24]. Biochar can be combusted as a pseudo-coal substitute for energy (e.g. in a combined heat and power unit) or applied to agricultural land as a soil amendment, aiding in water retention, soil quality, and boosting soil organic carbon levels [25-27]. Furthermore, fuel products from pyrolytic systems avoid the ‘blend wall’ barrier of ethanol integration into gasoline and diesel, thus enabling a transition to 100% renewable fuel without requiring a shift in vehicle fleet engine technology to accommodate ethanol [28]. Thermochemical catalytic upgrading of bio-oil products can also produce higher quality fuel products (e.g. aviation fuel) as well as bio-based commodity and specialty chemicals, which typically improve plant economics [29]. Despite all these advances and advantages over first generation fuels, pyrolysis still suffers from issues of reactor selectivity, high yield of light alkanes, low C<sub>6</sub>+ liquid carbon yield, and high hydrogen consumption all hinder the commercial implementation and environmental performance of single-stage fast pyrolysis [23]. As an alternative, Herron et. al and others have begun to develop multi-stage torrefaction systems, consisting of discrete thermal stages tuned to sequentially target the decomposition of hemicellulose, cellulose, and lignin fractions [30]. This specificity in targeting results in a dramatic improvement in liquid carbon yield, and allows for highly tailored catalytic upgrading strategies for each distinct, fractional bio-oil stream. Upgrading fractionated bio-oil streams via carbon-carbon (C-C) coupling reactions also tends to lower process hydrogen consumption, one of the factors influencing lifecycle environmental impacts. Furthermore, Zaines et al. proposed a multistage torrefaction to convert a poplar SWRC feedstock to fractionated bio-oil streams,

followed by catalytic upgrading to transportation-range biodiesel [31]. Results indicated 3.9x more C6+ liquid fuel than a fast pyrolysis base-case, with improved energy return on investment (EROI) as well as an 80% reduction in lifecycle GHG emissions compared to petroleum diesel. Furthermore, Winjobi et. al arrived at similar results, with an approximately 60% reduction in lifecycle GHG emissions for a similar two-step torrefaction and fast pyrolysis system [32].

While results for these multistage torrefaction systems show potential relative to single stage fast pyrolysis, real-world implementation is still hindered by the proposed plants' economic potential relative to standard crude oil [33]. One promising option to improve biorefinery profitability is to co-produce lucrative commodity and specialty chemicals, many of which are energy intensive and/or expensive to produce via petrochemical routes [34-36]. In 2014, the market value of cyclopentanone (CPO) was reported as ~\$15/kg, with global demand valued at \$100 million and expected to grow to \$130 million by 2020 – nearly 9000 metric tons at the given price [37]. CPO is a readily biodegradable, intermediate chemical used in the production of rubber chemicals, insecticides, electronics, pharmaceuticals, and perfumes/aromas [38], the latter two of which are its largest volume markets, projected for rapid growth in upcoming years [37]. Finally, due to the abundance of furfural in the multistage torrefaction system design of Zaines et. al. [39], it is feasible to produce CPO via catalytic Pincatelli ring rearrangement [40], followed by separation for sale as a specialty chemical. Not only might co-production of fuels and chemicals improve plant economics, but it also stands to drastically improve lifecycle environmental performance of both the primary fuel products [41] and of chemicals traditionally produced via carbon-intensive pathways. In particular, biomass-based production of CPO has been shown to have reasonable economic viability [42], and has the potential to drastically reduce fossil primary energy ( $PE_{\text{fossil}}$ ) consumption and lifecycle GHG emissions compared to traditional CPO production from adipic acid.

Integral to evaluating claims of environmental sustainability and comparing renewable fuels against GHG reduction standards is the necessity of performing holistic, systems-level lifecycle assessments (LCA) of entire supply chains, often also including the markets they would enter into. LCA serves to quantify resource extractions from the environment, transformations of

resources into products and further products, and emissions to the environment associated with some product or service, either on its own or in comparison to something offering a similar function [43]. Resource flows, product flows, and emissions are tracked via lifecycle inventory (LCI) databases across the entirety of any number of supply chains associated with the product or service of interest. In the event that a certain process produces multiple useful products, LCA practitioners must perform either a system boundary expansion or one of multiple types of allocation, depending on the conditions of the study and functionalities of the co-products. Finally, the International Organization for Standardization (ISO) has published standards for LCAs, stipulating the acceptable structures and methodologies of studies, the necessary types of data, and the proper layout and scope of documentation necessary to publish one's work [43].

Many next-generation biofuels currently under investigation have yet to reach technological maturity, and thus require forward-looking “prospective” or “anticipatory” assessments to evaluate their expected environmental and economic performances [44]. In attempting to estimate best-case or worst-case environmental performances of a product or service system, researchers can then offer comparisons against an existing baseline system to screen alternative technologies for their potential lifecycle environmental implications. Such assessments often also require chemical process design and modeling work, which has traditionally sought out economic optima on which to base the construction and operation of refineries and chemical plants. However, in light of the severity and time sensitivity of modern environmental challenges, some researchers have begun to search for environmental optima in addition to economic considerations [45, 46]. As learned from previous incentives for biofuel production (i.e. for corn ethanol), these analyses must contain quantitative rigor and statistical validity to ensure that alternative fuels are in fact environmentally and economically viable,

without simply offering the appearance of such traits [16, 17]. In an era where the climate clock ticks at such a severe pace, time is of the essence, and mistakes in planning the trajectory of energy technologies may have a higher cost to humanity than in years past.

In light of these challenges and opportunities, this work seeks to develop a consistent framework to quantify the lifecycle environmental performance of the co-production of emerging biofuels and bio-based chemicals, including rigorous systems-level process simulation coupled with a well-to-wheel (WTW) prospective LCA. Three CPO co-production design cases are established, for which process-scale and lifecycle environmental performances are evaluated via an array of both process and LCA metrics – including fossil Energy Return on Investment ( $EROI_{\text{fossil}}$ ) and lifecycle GHG emissions – allowing for comparison among cases and against baseline petroleum diesel. LCA metrics are calculated for multiple allocation methods, as well as two biochar co-product scenarios, to observe the implications of their established influence on these metrics [47, 48]. Finally, percentile values for said metrics are generated with statistical bootstrapping via Monte Carlo simulation to provide estimates of uncertainty, and sensitivity analysis is performed to quantify the dependence of LCA metrics on changes in input parameters.

Furthermore, this thesis specifically addresses the following set of research questions relating to the lifecycle environmental performance of a model biorefinery:

1. How does the co-production of bio-based specialty or commodity chemicals affect the WTW lifecycle GHG emissions and fossil EROI associated with the production of a drop-in biodiesel product? Does the primary fuel product produce low enough lifecycle GHG emissions to qualify for a production tax credit, and is fossil EROI significantly higher than unity?

2. How do these findings vary across co-product scenarios and allocation methods?

Which unit processes and model parameters contribute most to the environmental impacts?

3. Is such a study of co-producing fuels and chemicals comparable with existing LCAs of biofuels, and if not what barriers to standardization exist?

In addressing these questions, this thesis is arranged into five chapters, beginning with this introductory section to provide field-specific background information. Chapter two then goes on to detail the methodologies, data sources, and model scope considerations inherent in the chemical process modeling efforts. Chapter three proceeds to establish a mathematical framework for coupling process-level information with a lifecycle inventory model, while also providing information on the chosen methods and data sources. Chapter four serves to assimilate both the process modeling and LCA results, and begin to discuss their significance relative to the viability of the entire study. Chapter five then offers concluding remarks on methodological limitations and areas for future work, followed by a final list of works cited.

Components of each chapter are based on (1) an article currently under review, submitted to *ACS Sustainable Chemistry & Engineering*, and (2) a peer-reviewed article published in *Energy and Environmental Science*, with the citations:

1. Beck, A.W.; O'Brien, A. J.; Zames, G. G.; Resasco, D. E.; Crossley, S. P.; Khanna, V., *Systems-level Analysis of Energy and Greenhouse Gas Emissions for Co-Producing Bio-based Fuels and Chemicals: Implications for Sustainability*. Submitted to *ACS Sustainable Chemistry & Engineering*, October 2017.

2. Zaimes, G. G., Beck, A. W.; Janupala, R. R.; Resasco, D. E.; Crossley, S. P.; Lobban, L. L.; Khanna, V., *Multistage Torrefaction of Biomass and in-situ Catalytic Upgrading to Hydrocarbon Biofuels: analysis of life cycle energy use and greenhouse gas emissions*. Resubmission to Energy and Environmental Science, 2017. **10**(5): p. 1034-1050

Not included in this thesis, but also carried out under the direction of Dr. Vikas Khanna during my degree work, the following additional article is pending submission:

3. Beck, A. W.; Ng, C. A.; Khanna, V., *Evolution and Robustness of the Global Agricultural-Phosphorus Trade Network*. Submitting to Proceedings of the National Academy of Sciences, December 2017.

## **2.0 PROCESS DESIGN AND MODELING**

### **2.1 PROCESS DESCRIPTION**

The process flow diagram in Figure 1 illustrates lifecycle input and output flows crossing the system boundary as well as intermediate material flows for unit operations within it. Processes modeled within the system boundary include (1) an SRWC agricultural model, (2) a pretreatment facility, and (3) a theoretical, technologically mature “nth” multi-stage torrefaction biorefinery, operating on a basis of 2000 dry metric tonnes (DMT) of SRWC biomass per day. Agricultural modeling – including SRWC cultivation and harvesting, biomass storage, and direct land-use change (dLUC) – are derived from previous work to allow for the comparison of co-production of biofuels and biochemical with the strict production of only biofuels [39].

The multistage system in this work upgrades bio-oil fractions from two staged thermal decomposition reactors, sequentially operating at 360°C and 500°C, followed by catalytic upgrading pathways tailored to the bio-oil compositions of each effluent stream. Experimental yield data for a three-stage torrefaction system is given in Table 1, but represented here as two stages by combining the bio-oil streams of the first and second experimental stages, due to their constituent compounds having complimentary upgrading strategies. As such, this work models one torrefaction stage operating at 360°C and one 500°C pyrolysis stage to thermally decompose the dry, ash-free woody biomass.

**Table 1.** Yield values given as weight percentages of ash-free biomass input, for a bench-scale multistage torrefaction and pyrolysis system, representing bio-oil constituents via a set of model compounds [31].

<b>Product</b>	<b>Multistage Torrefaction and Pyrolysis</b>				<b>Single Stage Pyrolysis</b>
	<b>(wt%)</b>				<b>(wt%)</b>
	1 <sup>st</sup> Stage	2 <sup>nd</sup> Stage	Pyrolysis	Total	Total
H <sub>2</sub> O	9.20	6.80	0.00	16.00	13.20
Acetic Acid	6.06	2.09	0.45	8.60	9.28
Acetol	2.73	2.10	1.50	6.33	10.12
Furan	0.01	0.16	0.10	0.27	0.31
Furfural	4.65	4.43	0.63	9.71	5.49
Levoglucoosan	0.00	8.02	4.05	12.08	20.20
Toluene	0.00	0.75	0.26	1.01	0.40
Guaiacol	2.93	2.63	1.45	7.01	6.42
Cresol	0.04	0.93	0.33	1.30	1.29
Bio-Oil (Wet Basis)	25.61	27.91	8.78	62.30	66.69
Non-Condensable Gases	7.20	8.50	11.50	27.20	24.30
Biochar	0.00	0.00	10.50	10.50	9.01
Total	32.81	36.41	30.78	100.00	100.0

With respect to product categories, product compounds of C<sub>6</sub>+ chain-length are considered as suitable drop-in replacements for petroleum-derived liquid transportation fuel. Residual light hydrocarbons (C<sub>1</sub>-C<sub>5</sub>) are then separated and combusted to generate heat and electric utilities via an onsite CHP unit; remaining non-condensable gases (NCGs) are addressed via a combination of flaring and venting [39]. The biochar/ash co-product is also separated and utilized according to one of two co-product scenarios: combustion to generate utilities via said onsite CHP unit, or transportation to farms for use as a soil amendment. As illustrated in Figure 1, levoglucoosan is separated from the effluents of both torrefaction stages prior to upgrading, immediately mixed, and independently upgraded via hydrolysis and oxidation to produce gluconic acid. Gluconic acid then undergoes ketonization and is reintroduced to the bio-oil pool

in the hydrodeoxygenation (HDO) reactor. All upgraded fuel intermediates are sent to a final HDO reactor to remove oxygenated constituents, resulting in a wide array of vehicle-compatible biofuel products.

With respect to bio-based chemical production, three process-scale CPO co-production scenarios are investigated in this study. The first scenario, referred to as the Max CPO scenario, separates the maximum amount of CPO at 99% purity from the bio-oil pool through a staged distillation column train following the Piancatelli rearrangement reactor block. The Market CPO scenario separates ~20% of the produced CPO, thus exporting an amount equivalent to the estimated annual CPO market demand of 9000 metric tons in 2020, with a 90% stream rate [37]. The final scenario, named Max Fuel, produces the maximum amount of fuel by upgrading all converted CPO to C6+ transportation-range fuel via aldol condensation and HDO.

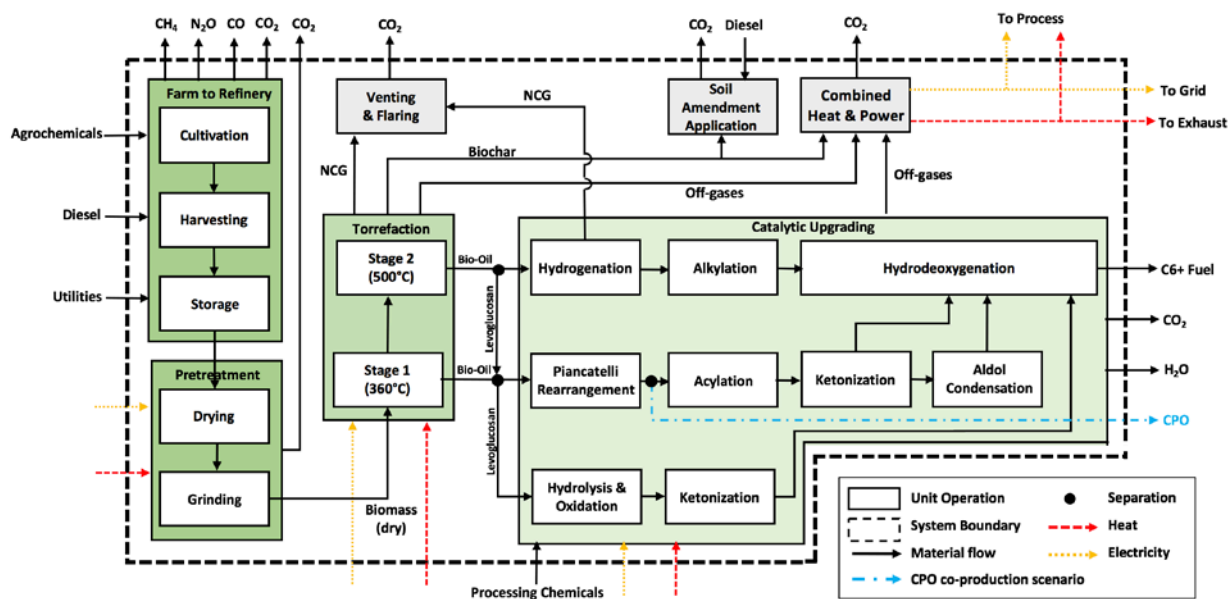


**Figure 1.** Process flow diagram containing SRWC agricultural modules [39], pre-treatment processing steps, and the full sets of thermal decomposition and catalytic upgrading unit operations in the biorefinery model. Heat and electricity flows from the combined heat and power (CHP) unit are consumed within the system boundary according to utility demands; only excess electricity is exported as a co-product.

## 2.2 UPGRADING CHEMISTRIES

A model compound approach is utilized to represent complex real-world mixtures of bio-oil constituents in terms of their most prominent molecular components, and is consistent with methods of prior studies [49-52]. As per the experimental yield data given in Table 1, seven groupings of torrefaction bio-oil product compounds are considered here as model compounds: carboxylic acids as acetic acid, light oxygenates as acetol, furanics as furan and furfural, aromatics as toluene, multifunctional phenolics as guaiacol, alkylated phenolics as *m*-cresol, and anhydrous sugars as levoglucosan. As mentioned above, these compounds are taken to be produced by an aggregated two stage torrefaction system, for which hourly yield values of bio-

oil compounds are given in Figure 2. Yield mass flow values result from the above weight percentage data and an assumed basis of 2000 DMT per day of ash-free SRWC biomass input.

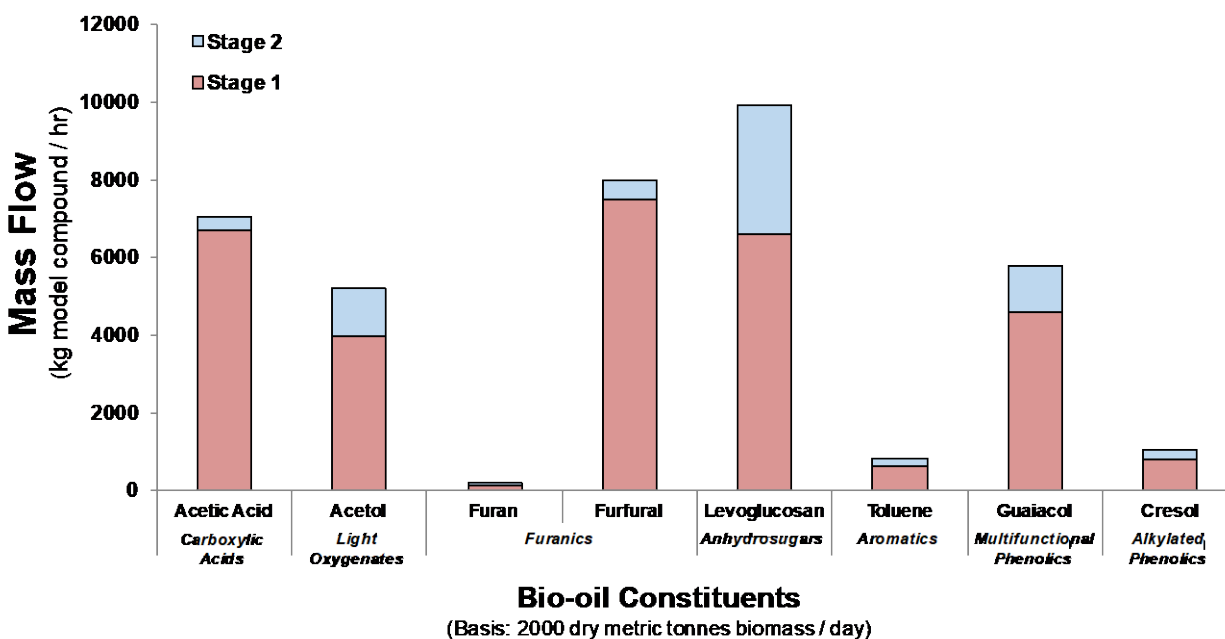
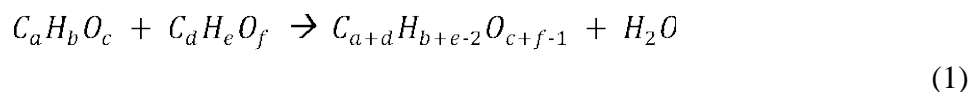


**Figure 2.** Torrefaction bio-oil yield distribution of model compound families.

These model compounds are then converted to C6+ transportation fuels and specialty chemical via a host of upgrading chemistries, including ketonization, alkylation, hydrolysis and oxidation, hydrogenation, and hydrodeoxygenation (HDO) [30]. Expanding on the multistage torrefaction and catalytic upgrading model of Zaines et al. [39] two additional carbon-carbon (C-C) coupling reaction pathways are investigated in this work: acylation and aldol condensation [30]. Acylation, an acid-catalyzed C-C coupling reaction with high selectivity towards carboxylic acid and aromatic compound coupling, enables much of the acetic acid found in the first stage torrefaction product stream to integrate into larger hydrocarbon compounds. Aldol condensation, a base-catalyzed C-C coupling reaction amongst two carbonyl compounds,

facilitates the joining of acetone, acetol, and remaining CPO into larger hydrocarbons. Additionally, Piancatelli ring rearrangement is modeled here as the basis for converting furfural into CPO [53]. Various studies have now generated CPO from biomass furfural via Piancatelli rearrangement under reducing conditions, due to the mechanism's unique ability to remove the heteroatom oxygen constituent [40, 53]. While primarily serving to produce a valuable specialty chemical, Piancatelli rearrangement also provides process flexibility, insofar as CPO can act as a building block for C-C coupling reactions [53]. Stoichiometric reaction equations for each catalytic upgrading chemistry considered here are provided in generalized forms in Equations 1-15.

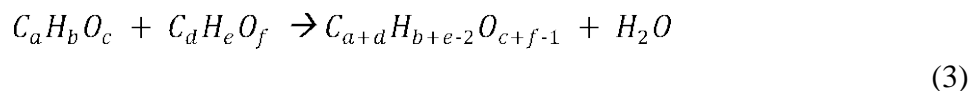
**Acylation.** Carbon-carbon coupling reaction of a carboxylic acid with aromatic compounds and furanics forming water as a by-product.



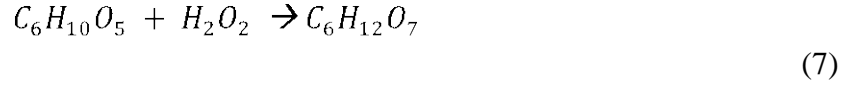
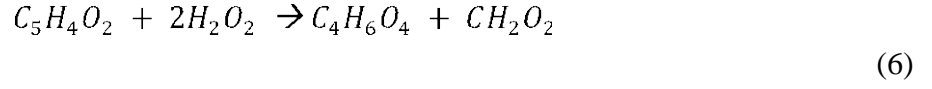
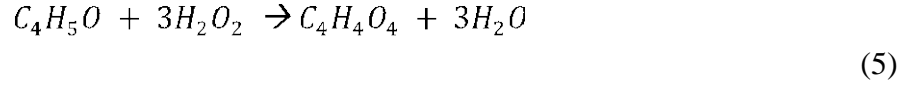
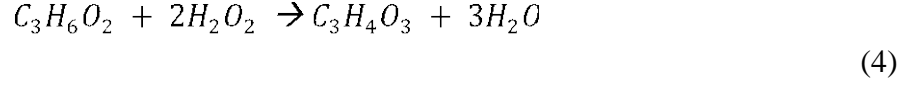
**Aldol Condensation.** Carbon-carbon coupling reaction of low carbon number species generating a dehydrated enone and water.



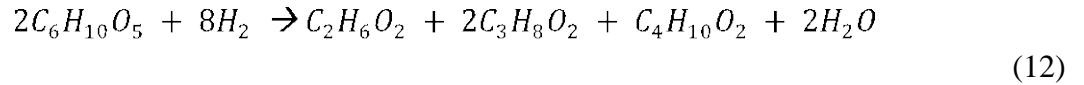
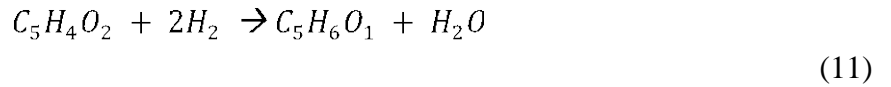
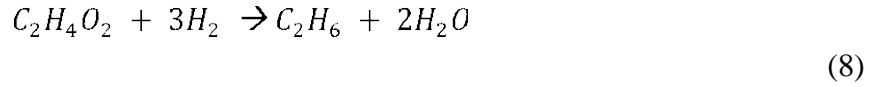
**Alkylation.** Carbon-carbon coupling reaction of an alcohol with aromatic compounds and furanics forming water as a by-product.



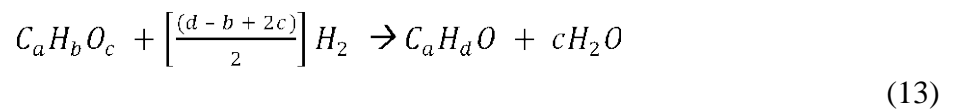
**Hydrolysis and Oxidation.** Oxidizing agents convert bio-oil compounds to carboxylic acids.



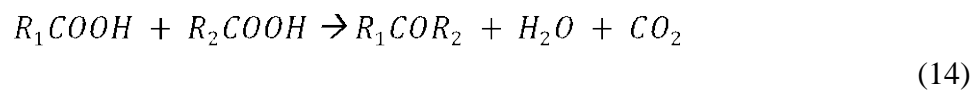
**Hydrogenation.** Mild hydro-processing conditions convert bio-oil compounds to stable intermediates (alkylating species).



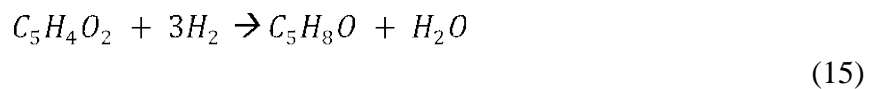
**Hydrodeoxygenation.** Removes oxygen constituents from bio-oil compounds through severe hydroprocessing and generates water.



**Ketonization.** Reaction between two carboxylic acids to produce a ketone, carbon dioxide, and water.



**Piancatelli Rearrangement.** Hydrogenation of furfural to general cyclopentanone and water.



## 2.3 CHEMICAL PROCESS MODELING

An Aspen Plus v10 model of the theoretical biorefinery was constructed to simulate the mass and energy flows necessary to conduct a prospective analysis. Experimental data from University of Oklahoma torrefaction and catalytic upgrading work are utilized in both representing torrefaction product yields and parametrizing the reactor blocks of the simulation [30, 53]. Additional details regarding experimental setup and data acquisition are provided by Zaines et al., 2017 and Herron et al., 2016 [30, 39]. As indicated above, the process simulation developed here includes only two torrefaction stages, operating at 360°C and 500°C. In estimating product yields, the UNIQUAC activity coefficient model is adopted, and applied to Aspen equilibrium reactor blocks to generate steady-state yields for the given reaction pathways. Material properties data for all model compounds are estimated via the National Institute of Science and Technology ThermoData Engine (NIST-TDE). Detailed Aspen flowsheet images are provided in Figures 3-5, for which comprehensive stream summary information is attached as set of spreadsheets, and may be used to identify stream compositions and physical properties via identifiers in the flowsheets.

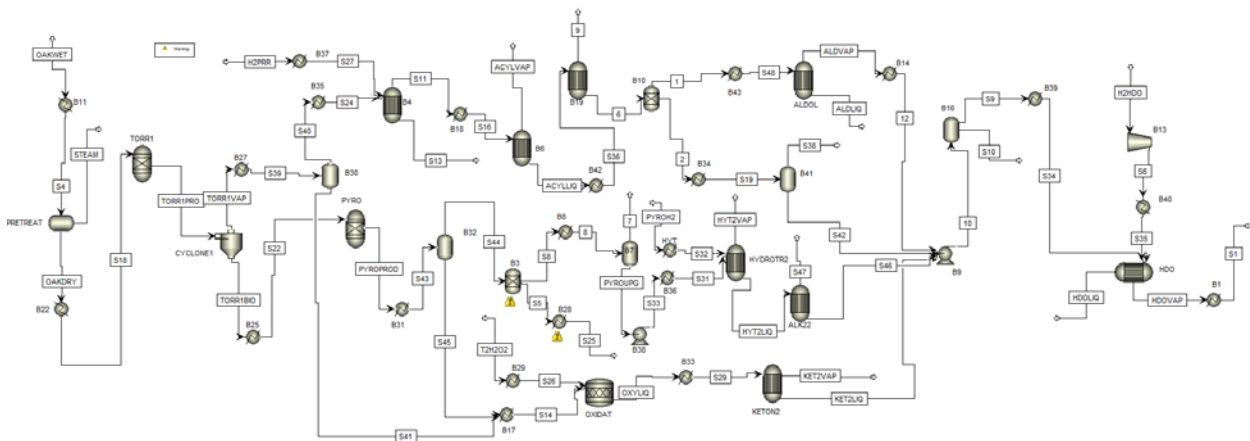
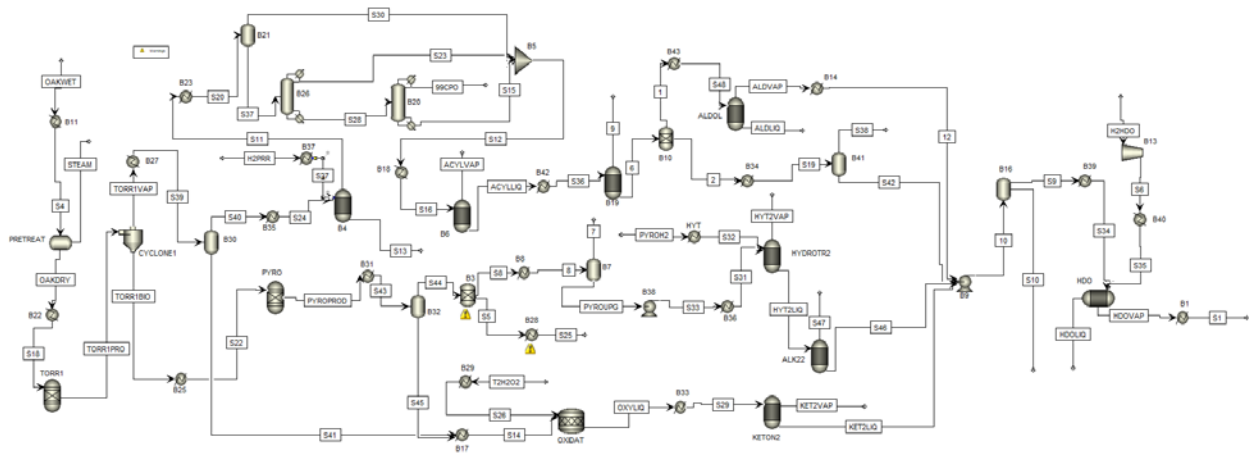
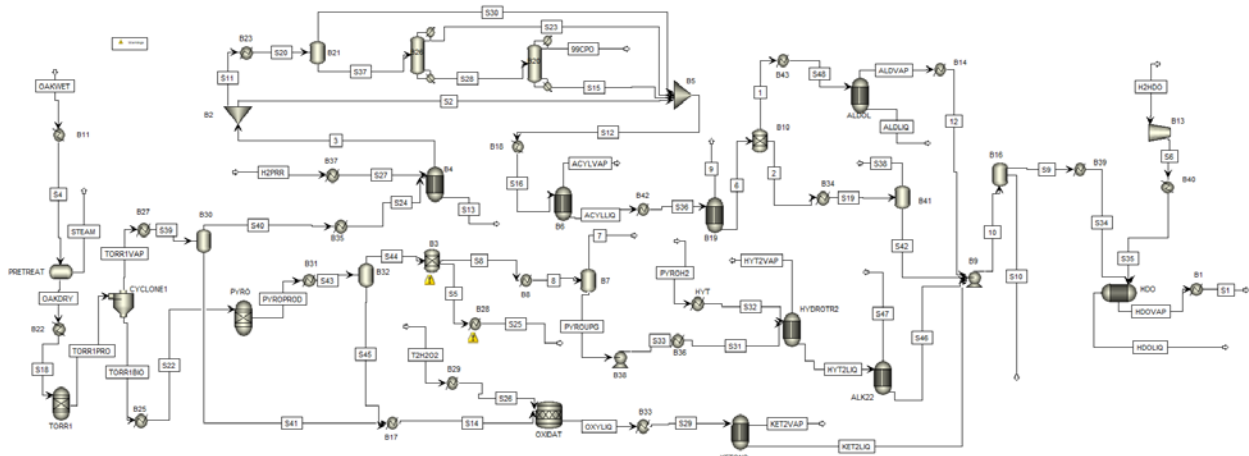


Figure 3. Aspen process simulation layout for Max Fuel Scenario



**Figure 4.** Aspen process simulation layout for Max CPO Scenario



**Figure 5.** Aspen process simulation layout for Market CPO Scenario.

Heat and pressure conditioning unit operations are included before each reactor to establish appropriate inlet conditions and provide a more realistic set of plant utility requirements. Graphical pinch analysis is used to estimate the minimum total heating and cooling duties, wherein certain stream enthalpy values were determined via linear estimation of enthalpy vs temperature graphs, to account for the complex latent and sensible heating characteristics of

multiphase, multi-component streams. A minimum pinch temperature of 10°C is assumed and used to generate the hot and cold composite curves plotted in Figures 6, 7, and 8, from which minimum heating and cooling duties are also derived.

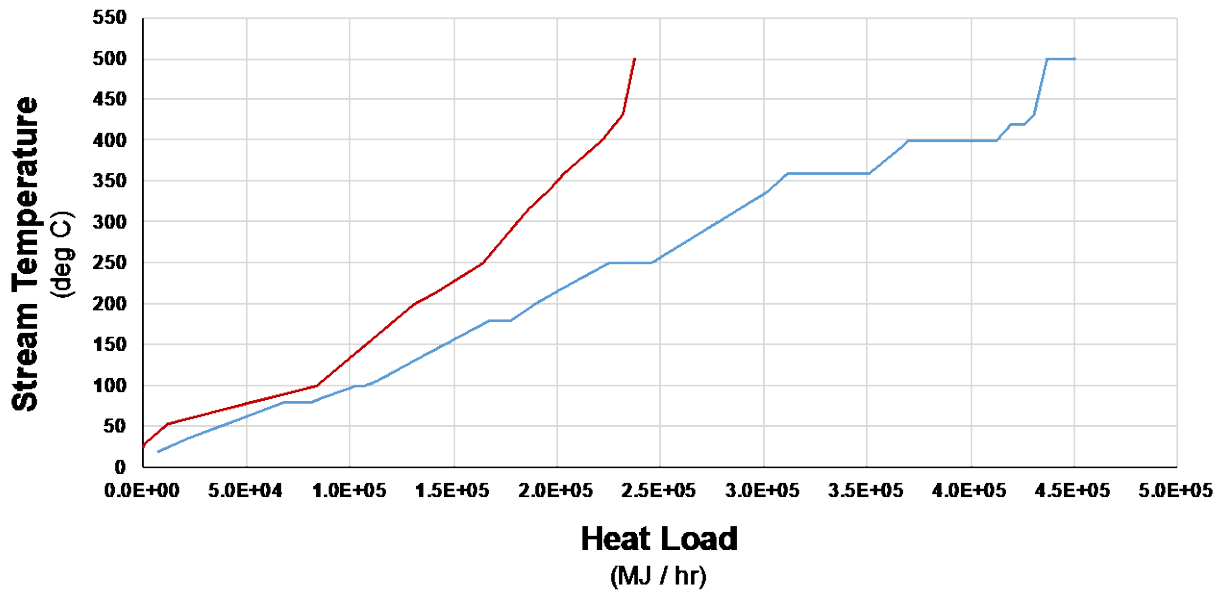


Figure 6. Temperature versus enthalpy pinch analysis plots, depicting hot (red) and cold (blue) composite curves for the Max CPO co-production case.

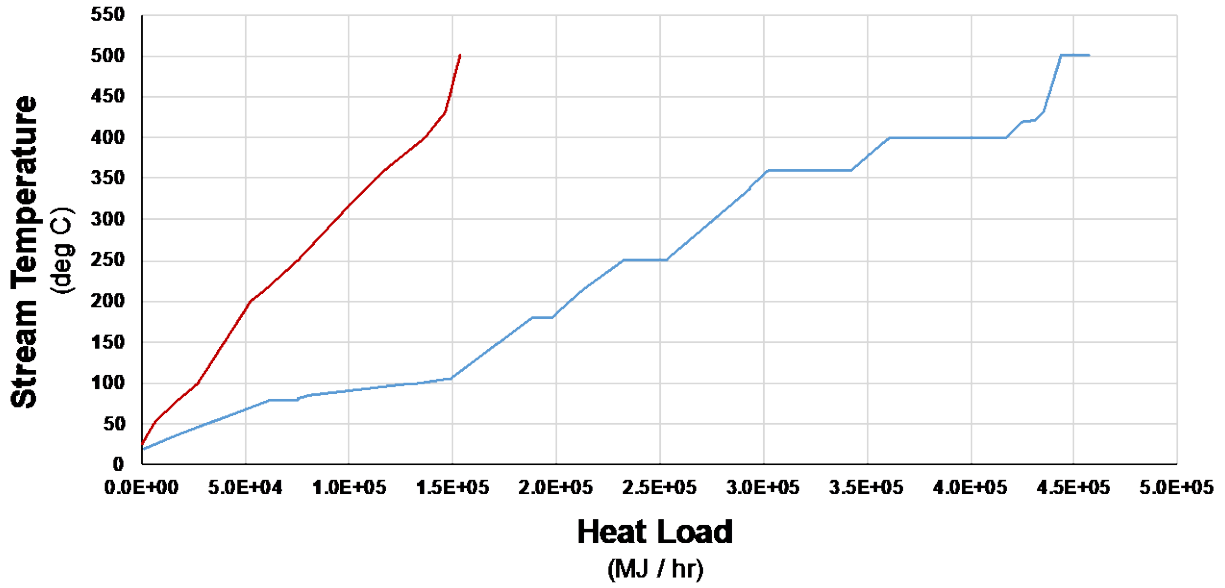


Figure 7. Temperature versus enthalpy pinch analysis plots, depicting hot (red) and cold (blue) composite curves for the Market CPO co-production case.

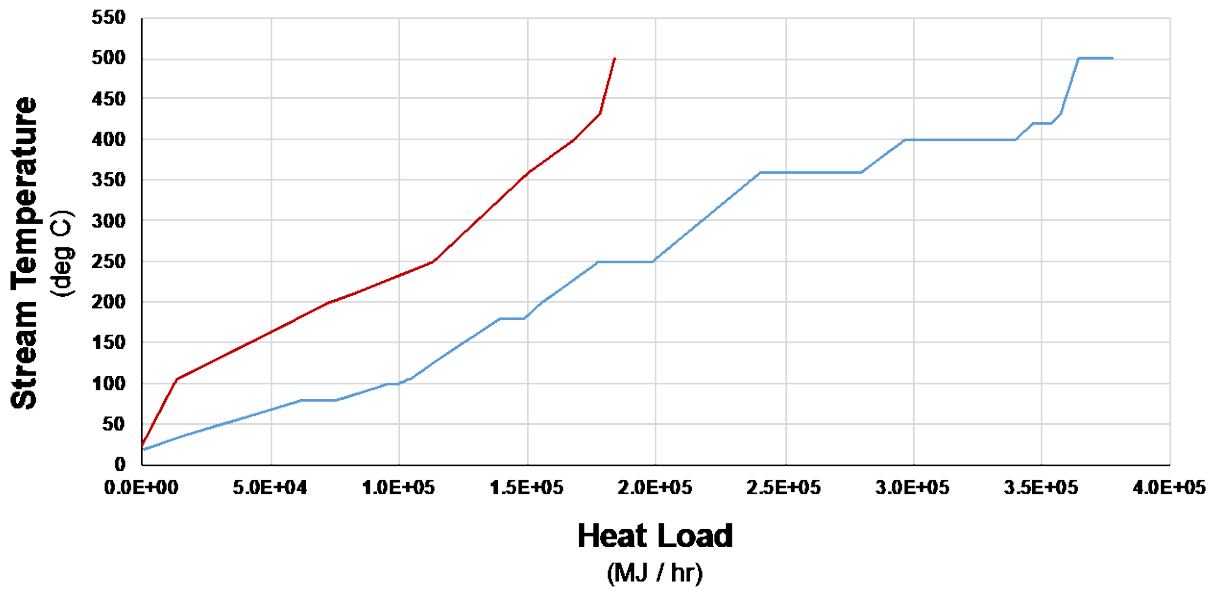


Figure 8. Temperature versus enthalpy pinch analysis plots, depicting hot (red) and cold (blue) composite curves for the Max Fuel co-production case.

The full array of biorefinery utility requirements are provided in Table 2, including all heat and electricity requirements dictated by temperature and pressure conditioning operations. Pretreatment electricity consumption – primary consisting of chopping and grinding – is derived via a regression model developed by Miao et. al, 2011[54]. Compression and pumping electricity requirements are extracted directly from Aspen Plus, where each reactor inlet stream has both a pressure and temperature conditioning operation to meet reactor conditions. Pumping requirements also include values for the pumping of cooling water, which is calculated via a set of two energy balance equations, given as Equations 16 and 17:

$$\dot{Q}_{cooling} = \dot{m}_{CW} C_p \Delta T \quad (16)$$

$$\dot{W}_{pump} = \frac{1}{\epsilon} \dot{V} \Delta P \quad (17)$$

The net cooling duty  $Q_{cooling}$  (MJ / hr) is assumed to be delivered via cooling water at a steady-state temperature differential  $\Delta T$  of 10°C, which are used with the heat capacity of water (4.184 kJ / kg°C) to solve for the required cooling water mass flow rate  $m_{CW}$  (kg / hr). Pumping power  $W_{pump}$  (MJ / hr) is then calculated via the flow work expression  $V\Delta P$  (MJ / hr), adjusted for an assumed pumping  $\epsilon$  efficiency of 75%. The cooling water volumetric flow rate  $V$  is simply calculated by dividing the mass flow rate by the density of water. Total pressure drop – including estimates for pipe head losses (15psi), control valve losses (10psi), static head losses (8.7psi), and exchanger losses (5psi) – is estimated at approximately 38.7psi for the full cooling water loop, including an assumed average cooling tower height of 20ft. for static losses. The final cooling water pumping requirements  $W_{pump}$  are then added to the pumping requirements of the Aspen flowsheet, and presented as the aggregate ‘Pumps’ category in Table 2. Integrated plant

utility requirements are an essential component of formulating a realistic prospective chemical process model and providing information for the lifecycle inventory and impact assessment steps.

**Table 2.** Total process utility requirements for all CPO co-production scenarios, including electricity and heat demands from pressure and temperature conditioning unit operations. Minimum heating and cooling duties are calculated via pinch analysis, and electricity values are acquired from Aspen v10 simulation results.

<b>Utility Requirement</b>	<b>Unit</b>	<b>Max CPO</b>	<b>Market CPO</b>	<b>Max Fuel</b>
Pretreatment	Electricity (MJ/hr)	59.7	59.7	59.7
Compressors	Electricity (MJ/hr)	2302.6	2571.6	2626.6
Pumps	Electricity (MJ/hr)	403.6	385.0	391.5
Minimum Heating Utility	Heat (MJ/hr)	213681.7	303169.8	194238.5
Minimum Cooling Utility	Heat (MJ/hr)	6809.6	763.5	665.2

Finally, with respect to separations, before entering the primary column in CPO co-production scenarios, the Piancatelli reactor effluent stream was cooled to 35°C and light compounds were removed and returned to the upgrading process via flash separation, thereby reducing the energy and size requirements of the distillation columns. Streams with inseparable or negligible CPO leaving columns were returned to the upgrading process. Distillation column key components – between which the first column is designed to split the feed stream into two groups of compounds based on their relative volatilities – were selected by graphical analysis of stream components’ vapor pressure vs. temperature graph provided by Aspen and shown in Figure 9. Following these design steps, values for process mass and energy input and output flows are coupled to their associated products and processes within the lifecycle inventory model, and used in calculating process performance metrics to compare to LCA results.

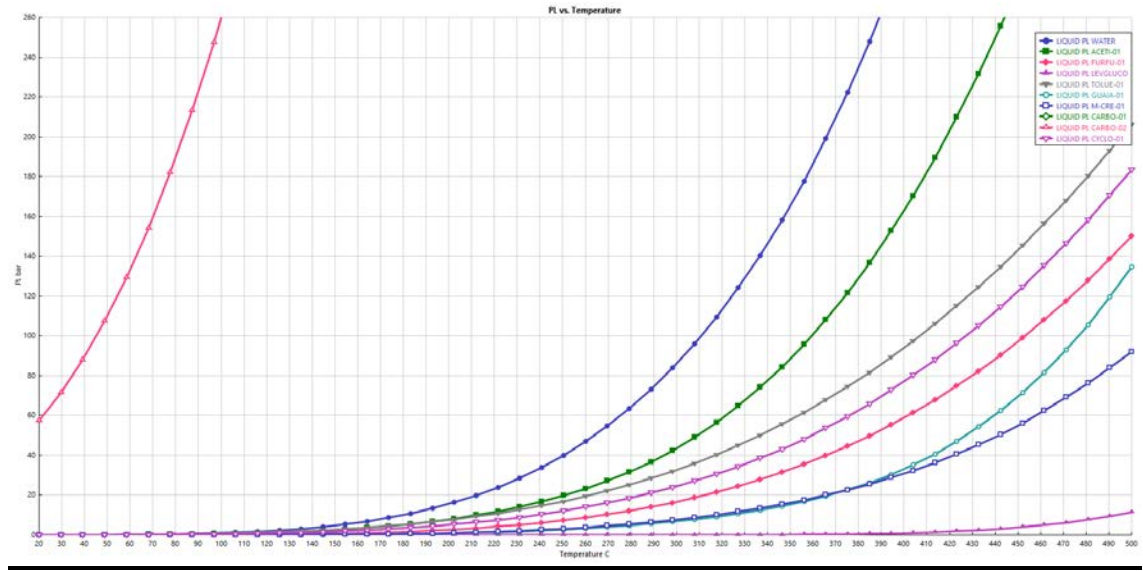


**Figure 9.** Vapor pressure versus temperature curves for compounds entering the first CPO-separating distillation column, used to assign light and heavy column keys. Toluene (grey) is taken as the light key, and cyclopentanone (magenta, hollow del symbol) as the heavy key.

### **3.0 LIFECYCLE ASSESSMENT STUDY DESIGN**

#### **3.1 LIFECYCLE GOAL AND SCOPE**

A well-to-wheel LCA model is developed to compare the lifecycle GHG emissions profiles and energy return on primary fossil energy investment ( $EROI_{\text{fossil}}$ ) of a poplar SRWC-fed biorefinery via three biofuel and biochemical co-production design cases, as they relate to each other and to baseline petroleum diesel. A functional unit of 1 MJ of liquid transportation fuel is selected for comparability across previous studies [32, 39]. A process flow diagram is given above in Figure 1, containing aggregated unit processes and the lifecycle system boundary, within which various adjustments are made to the scope of this study: Due to a negligible contribution to overall environmental impact, inventory data and modeling for capital equipment and infrastructure are excluded from this analysis [55, 56]. Conversely, the lifecycle impacts of catalyst requirements cannot be neglected [57], and are estimated via Ecoinvent data for zeolite powder, in accordance with previous work [58]. We also assume that residual heating utilities – often generated in excess by certain co-product scenarios – cannot be exported for co-product credit, as this biorefinery model is assumed to be isolated from other industrial operations.

### **3.2 LIFECYCLE INVENTORY, IMPACT MODELING, AND CO-PRODUCT HANDLING**

Lifecycle data from the EcoInvent 3.4 database – for which metadata is provided in Table 3 – is employed in constructing the Lifecycle Inventory (LCI), and Intergovernmental Panel for Climate Change (IPCC) 100-year time horizon global warming potential (GWP) values and Cumulative Energy Demand (CED) characterization factors are used to quantify lifecycle GHG emissions and primary fossil energy consumption, respectively [59-61]. More specifically, impact factors from IPCC 2013 GWP 100a v1.01 and Cumulative Energy Demand v1.09, shown in Table 3 as ‘IPCC 2013’ and ‘CED v1.09’ respectively, are employed.

**Table 3.** Lifecycle unit process and impact factor data sources, also including confidence interval information and sample size  $N$  accessed (if available) [61].

<b>Unit Process Description</b>	<b>Unit</b>	<b>Database</b>	<b>Method</b>	<b>C.I.</b>	<b>N</b>
Diesel (RoW) market for   Alloc Def U	kg	Ecoinvent 3.4	IPCC 2013	95%	10 <sup>4</sup>
Diesel (RoW) market for   Alloc Def U	kg	Ecoinvent 3.4	CED v1.09	95%	10 <sup>4</sup>
Transport, freight, lorry > 32 metric tons, EURO5 (ROW)   Alloc Def U	tkm	Ecoinvent 3.4	IPCC 2013	95%	10 <sup>3</sup>
Transport, freight, lorry > 32 metric tons, EURO5 (ROW)   Alloc Def U	tkm	Ecoinvent 3.4	CED v1.09	95%	10 <sup>4</sup>
Electricity, High Voltage U.S.   Production Mix   Alloc, Def U	MJ	Ecoinvent 3.4	IPCC 2013	95%	10 <sup>4</sup>
Electricity, High Voltage U.S.   Production Mix   Alloc, Def U	MJ	Ecoinvent 3.4	CED v1.09	95%	10 <sup>4</sup>
Zeolite, powder (RER)   Production   Alloc Def U	kg	Ecoinvent 3.4	IPCC 2013	N/A	N/A
Zeolite, powder (RER)   Production   Alloc Def U	kg	Ecoinvent 3.4	CED v1.09	N/A	N/A
Hydrogen (reformer) E	kg	Industry data 2.0	IPCC 2013	N/A	N/A
Hydrogen (reformer) E	kg	Industry data 2.0	CED v1.09	N/A	N/A
Heat, natural gas, at industrial furnace >100 kW/RER U	MJ	Ecoinvent 3.4	IPCC 2013	95%	10 <sup>4</sup>
Heat, natural gas, at industrial furnace >100 kW/RER U	MJ	Ecoinvent 3.4	CED v1.09	95%	10 <sup>4</sup>
Hydrogen peroxide, without water, in 50% solution state (RER)   hydrogen peroxide production, product in 50% solution state   Alloc Def, U	kg	Ecoinvent 3.4	IPCC 2013	95%	10 <sup>4</sup>
Hydrogen peroxide, without water, in 50% solution state (RER)   hydrogen peroxide production, product in 50% solution state   Alloc Def, U	kg	Ecoinvent 3.4	CED v1.09	95%	10 <sup>4</sup>
Transport, freight, inland waterways, barge (RER)  processing  Alloc Def, U	tkm	Ecoinvent 3.4	IPCC 2013	95%	10 <sup>4</sup>
Transport, freight, inland waterways, barge (RER)  processing  Alloc Def, U	tkm	Ecoinvent 3.4	CED v1.09	95%	10 <sup>4</sup>
Transport, freight train (US)  diesel  Alloc Def, U	tkm	Ecoinvent 3.4	IPCC 2013	95%	10 <sup>4</sup>
Transport, freight train (US)  diesel  Alloc Def, U	tkm	Ecoinvent 3.4	CED v1.09	95%	10 <sup>4</sup>
2-cyclopentone (RoW)  decarboxylative cyclization of adipic acid   Alloc Def, S	kg	Ecoinvent 3.4	IPCC 2013	N/A	N/A
2-cyclopentone (RoW)  decarboxylative cyclization of adipic acid   Alloc Def, S	kg	Ecoinvent 3.4	CED v1.09	N/A	N/A

As developed by Zaines et al., an SRWC production model for poplar – including biomass cultivation and harvesting, short-term storage, farm-to-refinery transportation, and dLUC impacts – serves as input to the novel ASPEN process model described above [39]. The chemical process model then converts the specified material inputs into an array of feasible product outputs, while also specifying heat-integrated utility requirements and whether net import or export as a co-product of electricity occurs. Three different CPO co-production and two biochar co-product scenarios are considered, resulting in six total co-product permutations. The biochar scenarios include (1) application as a soil amendment, and (2) combustion as a fuel source in a combined heat and power (CHP) unit process, both of which are further detailed in the aforementioned paper [39].

Based on the varied end-uses of the biofuel, CPO, and electricity co-products, market-based allocation and displacement were selected as allocation methods. Commodity prices of each product for market allocation can be found in the Table 4, discussed in further detail below. Whereas market-based allocation apportions environmental impacts based on the proportion of revenue streams (\$USD) associated with each co-product, the displacement method must assign a primary product – consistently the biofuel in this study – and claim a negative credit for displacing some quantity of CPO and/or the average grid-mix of U.S. electricity. Both products of combusting excess light hydrocarbons (C1-C5) and conditionally biochar as well, all heat produced by the CHP unit is treated as remaining within the product system, while net-electricity exports may leave as a co-product. Application of biochar as a soil amendment also necessitates a negative GHG credit, and is incorporated into the total emissions balance before co-product allocation or displacement methods are carried out.

### 3.3 LIFECYCLE IMPACT METRICS

Lifecycle GHG emissions, measured in grams of carbon dioxide equivalent (g CO<sub>2</sub>e), encapsulate all direct and indirect emissions of GHGs associated with the biofuel's WTW lifecycle. However, sequestration of carbon within the biomass via photosynthesis is not initially taken as a negative credit, allowing for all off-gases, non-condensable gases, and complete combustion byproducts of the biomass and its co-products to be considered carbon-neutral. Due to a lack of use phase and end-of-life data for CPO, it is assumed that all CPO produced will eventually degrade to CO<sub>2</sub> and re-enter the atmosphere. Combusting biochar via CHP follows the same logic, but application as a soil amendment results in a net carbon sequestration as soil-organic carbon, requiring a negative GHG credit while adjusting for a gradual re-release of some 20% of the initial carbon content over 100 years [47]. Error-bounded lifecycle GHG emissions are compared to the U.S. EPA's RFS2 thresholds of 50% lifecycle GHG reductions versus petroleum gasoline (~92.89 g CO<sub>2</sub>e/MJ-fuel) and/or diesel (~91.94 g CO<sub>2</sub>e/MJ-fuel) [5]. As the resultant threshold values are within >1 g CO<sub>2</sub>e/MJ-fuel, only the stricter threshold of diesel is visualized below. Fossil energy return on investment (EROI<sub>fossil</sub>) is defined as the heat energy contained within the liquid fuel (MJ) divided by the total primary fossil energy required to produce it (MJ-PE<sub>fossil</sub>); biofuel production pathways that yield an EROI value significantly greater than 1 are desirable, as they provide more heat energy as a final product than they require to reach that physical state.

$$EROI_{fossil} = \frac{\text{Fuel Energy (MJ)}}{\text{Primary Fossil Energy Invested (MJ)}} \quad (18)$$

### 3.4 UNCERTAINTY AND SENSITIVITY ANALYSIS

Monte Carlo simulations are carried out for a wide array of inventory data and parameters by either sampling randomly from probability density functions or bootstrapping, depending on available distribution information or datasets. Additional information on underlying probability distributions for model parameters can be found in Table 4, including model parameter units, family of distribution, and distribution parameters.

**Table 4.** Summary of LCI statistical metadata, including distribution types and parameter values. Statistical information for direct land use change, cuttings production, and woody biomass production modules are derived from and presented in Zaines et. al, 2017 [31].

<b>Parameter</b>	<b>Unit</b>	<b>Distribution</b>	<b>Min</b>	<b>Max</b>	<b>Peak Value</b>	<b>Point Est.</b>
<b><i>Local Transport</i></b>						
Transport Biomass (Farm-to-Refinery)	km	Triangular	50	150	100	-
<b><i>Fuel Conversion &amp; Upgrading</i></b>						
Weight Hourly Space Velocity	hr <sup>-1</sup>	Point Est.	-	-	-	0.2
Catalyst Lifetime	days	Uniform	60	365	-	-
<b><i>Fuel Transport and Distribution</i></b>						
Transport Biofuel (Refinery-to-Bulk Terminal) via Barge	miles	Point Est.	-	-	-	520
Transport Biofuel (Refinery-to-Bulk Terminal) via Rail	miles	Point Est.	-	-	-	800
Transport Biofuel (Refinery-to-Bulk Terminal) via Heavy Duty Truck	miles	Point Est.	-	-	-	50
Transportation Mix (Barge)	%	Point Est.	-	-	-	8%
Transportation Mix (Rail)	%	Point Est.	-	-	-	29%
Transportation Mix (Heavy Duty Truck)	%	Point Est.	-	-	-	63%
Transport Biofuel (Bulk Terminal-to-Refueling station)	miles	Point Est.	-	-	-	30

Table 4 (continued).

Parameter	Unit	Distribution	Min	Max	Peak Value	Point Est.
<b><i>Coproduct and Scenario Analysis</i></b>						
CHP – Heat Conv. Efficiency	(%)	Triangular	44%	48%	52%	-
CHP – Electrical Conv. Efficiency	(%)	Triangular	20%	35%	25%	-
Biochar Carbon Loss (to atm.)	(%C emitted)	Uniform	0%	20%	-	-
Transport Biochar (Refinery-to-Farm) via Heavy Duty Truck	km	Triangular	50	150	100	-
Diesel Use - Biochar land application	L ha <sup>-1</sup>	Triangular	0.9	4.7	2	-
Transport CPO (Refinery-to-Bulk Terminal) via Barge	miles	Point Est.	-	-	-	520
Transport CPO (Refinery-to-Bulk Terminal) via Rail	miles	Point Est.	-	-	-	800
Transport CPO (Refinery-to-Bulk Terminal) via Heavy Duty Truck	miles	Point Est.	-	-	-	50
CPO Transportation Mix (Barge)	%	Point Est.	-	-	-	8%
CPO Transportation Mix (Rail)	%	Point Est.	-	-	-	29%
CPO Transportation Mix (Heavy Duty Truck)	%	Point Est.	-	-	-	63%
<b><i>Co-product Prices</i></b>						
Diesel Price (Year-to-date monthly average, U.S.) [62]	\$/gal	Point Est.	-	-	-	2.581
Electricity Price (Year-to-date average, Industrial customer, U.S.) [63]	\$/kWh	Point Est.	-	-	-	0.0691
CPO Price [37]	\$/kg	Point Est.	-	-	-	15

Statistical approaches such as these serve to quantify and assist in visualizing the accumulated uncertainty across the lifecycle of a given product or service, and incorporate uncertainty into the LCA metrics we set out to compare. Sensitivity analyses are also performed on both lifecycle GHG emissions and  $EROI_{\text{fossil}}$ , under each co-product scenario and allocation scheme, by varying key process parameters by  $\pm 20\%$  to identify those that hold the strongest influence over said metrics.

## **4.0 RESULTS AND DISCUSSION**

### **4.1 PRODUCT DISTRIBUTION**

The product distributions for all fuel and CPO co-production scenarios are given in Figure 10. The Max CPO case shows significantly higher formation of C6 compounds, due to remaining light oxygenates (acetol and acetone) reacting to form C6 compounds via aldol condensation, whereas the acetol in the other scenarios favors primary and secondary C-C coupling reactions with residual CPO. As such, the Max CPO case also has lower C8 and C13 yields, since most of the CPO is removed upstream from the aldol condensation reactor. The high formation of C3 species compared to other light hydrocarbons (C2-C5) is attributed to unconverted light oxygenates (acetic acid, acetol, and acetone) under equilibrium conditions. All cases reported a consistency in C10 compounds due to reactions between acetol and toluene species in the acylation reactor; low levels of C10 products is attributed to the acylation reactor configuration for maximum C6+ output. While the Market CPO and Max Fuel scenarios display similar product distributions, the Market CPO case produces a high value-added product, thus allowing for potentially higher profitability in emerging bio-based energy technologies.

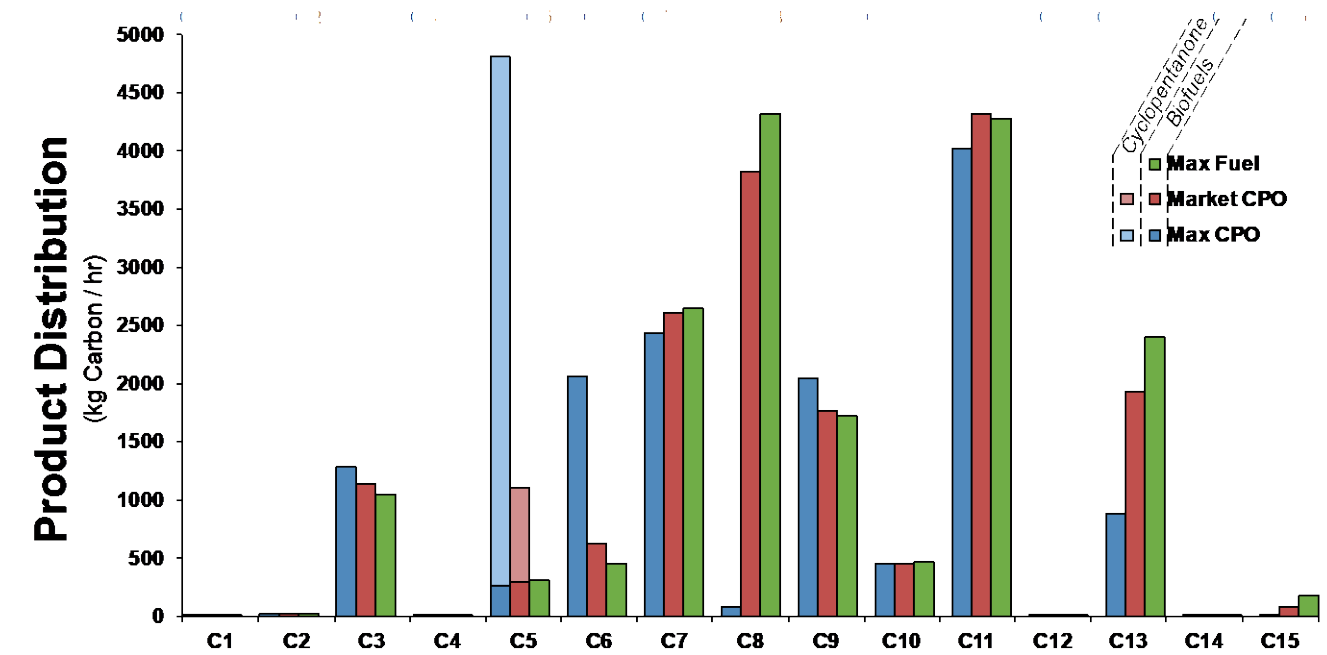


**Figure 10.** Product carbon distributions of fuel and CPO products (kg C / hr) in Max Fuel, Market CPO, and Max CPO scenarios. Lighter bars indicate quantities of CPO production, and darker bars indicate fuel. Compounds beyond C15 are not produced by any system.

## 4.2 PROCESS CARBON FLOWS

Looking now at the distribution of carbon within the process, Figure 11 represents the total carbon flows of the process simulation for the Market CPO case – chosen as a pseudo-average representation of the three cases. After the first 360°C torrefaction stage, approximately 45.5% of total biomass carbon ( $C_{\text{tot,biomass}}$ ) is upgraded through the sequential train of Piancatelli rearrangement, acylation, ketonization, and aldol condensation reactors. The remaining 54.5% is divided between two reactor inlets: the second 500°C pyrolysis stage (46.6%  $C_{\text{tot,biomass}}$ ) and a targeted levoglucosan pathway (7.9%  $C_{\text{tot,biomass}}$ ) comprising a sequence of oxidation and ketonization reactors. After thermochemical conversion of the 46.6%  $C_{\text{tot,biomass}}$  in the second

pyrolysis reactor, an additional 3.9%  $C_{\text{tot,biomass}}$  consisting of levoglucosan is separated and upgraded to fuel through its respective pathway. The remaining 5.3%  $C_{\text{tot,biomass}}$  is upgraded to fuel via hydrogenation and alkylation, and 27.9%  $C_{\text{tot,biomass}}$  is removed as biochar. The remaining pyrolysis effluent of 9.3%  $C_{\text{tot,biomass}}$  constitutes light hydrocarbons combusted in the CHP unit. All fuel upgrading pathways merge into the final HDO reactor, where 43.7%  $C_{\text{tot,biomass}}$  is upgraded to C6+ synthetic bio-oil and C1-C5 light alkanes. Furthermore, 45.8%  $C_{\text{tot,biomass}}$  is retained in final revenue-generating products (fuel and CPO), despite the removal of biochar, light hydrocarbons, and NCG waste-carbon throughout various reactors.

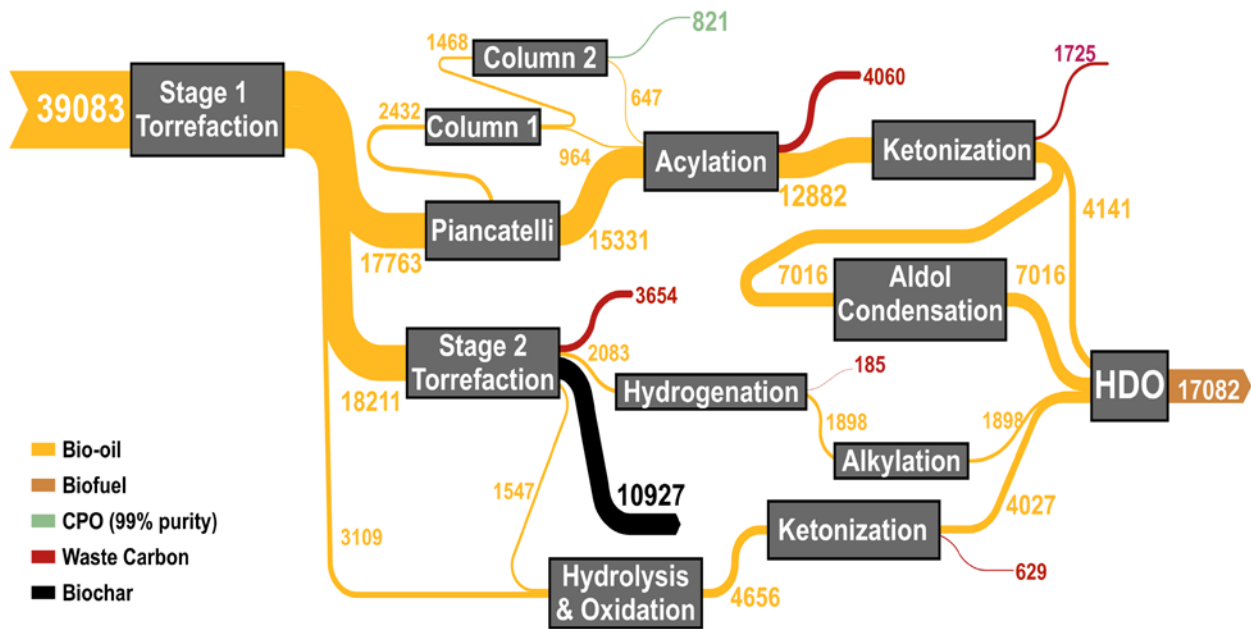


**Figure 11.** Process-level carbon flows (kg C / hr) for the Market CPO co-production scenario.

### 4.3 PROCESS-SCALE METRICS

An array process-level metrics, tabulated in Table 5, are used to compare performance across the different scenarios. All scenarios resulted in nearly equal effective carbon yield ( $\text{kg C}_{\text{products}} / \text{hr}$ ), calculated as the sum of C6+ Fuel Carbon Yield and Biochemical Carbon Yield. However, the Market CPO case produced a slightly lower value than Max Fuel due to the former's higher carbon-normalized flowrates of unconverted C2-C5 products (acetol, acetone, residual CPO) entering the HDO reactor, which are excluded from product carbon yields. All scenarios lowered hydrogen consumption ( $\text{kg H}_2 / \text{hr}$ ) by approximately 40% relative to single stage fast pyrolysis models of Zaines and co-authors [23, 39], and result in approximately equal effective carbon efficiencies of ~42%. The maximum CPO case produced the highest effective carbon yield to hydrogen consumption ratio of 7.55, due to substantial upstream removal of CPO and subsequent reduced hydrogenation requirements. This finding is confirmed via comparison with the Market CPO case, which has an ~0.5 lower effective carbon yield to hydrogen consumption ratio, yet both Market and Max CPO scenarios have nearly equal effective carbon yields. Additionally, C6+ Fuel Carbon Yield for Market CPO and Max Fuel scenarios are very similar, despite the Market CPO case producing a high-value co-product. These findings suggest that, insofar as markets allow, removing marketable bio-chemicals upstream can reduce hydrogen consumption, and other forms of downstream processing, without excessive loss in fuel production – an integral step towards commercially feasible bio-based fuel and chemical technologies.

**Table 5.** Yield- and efficiency-oriented process performance metrics for each co-production scenario.

<b>Process Performance Metrics</b>	<b>Max CPO</b>	<b>Market CPO</b>	<b>Max Fuel</b>
<b>Absolute Fuel Yield</b> (kg C <sub>6+</sub> Fuel / hr)	14203	18343	19326
<b>C<sub>6+</sub> Fuel Carbon Yield</b> (kg C <sub>C<sub>6+</sub> Fuel</sub> / hr)	11987	15599	16456
<b>Biochemical Carbon Yield</b> (kg C <sub>CPO</sub> / hr)	4553	815	0
<b>Effective Carbon Yield</b> (kg C <sub>products</sub> / hr)	16540	16413	16456
<b>Hydrogen Consumption</b> (kg H <sub>2</sub> / hr)	2191	2362	2397
<b>Effective Carbon-Yield-to- Hydrogen-Consumption Ratio</b> (kg C <sub>products</sub> / kg H <sub>2</sub> )	7.55	6.95	6.87
<b>Effective Carbon Efficiency</b> (kg C <sub>products</sub> / kg C <sub>Biomass</sub> ) x 100)	42.3	42.0	42.1

#### 4.4 LIFECYCLE GHG EMISSIONS AND EROI

Lifecycle GHG emissions and EROI<sub>fossil</sub> values for the primary biofuel product stream are provided in Figure 12 as box plots, chosen due to the skewness and asymmetry of the metrics' underlying distributions. Percentile values are shown across CPO co-production and biochar co-product scenarios, and are plotted against threshold values for each metric: the RFS2 50% diesel GHG reduction threshold of 45.97 g CO<sub>2e</sub>/MJ-fuel – calculated as 50% of 91.94 g CO<sub>2e</sub>/MJ-diesel, below which fuels qualify for tax credit – and an EROI<sub>fossil</sub> value of 1, which fuels should surpass to provide a net energy gain. The median biofuel GHG values, also presented numerically in Table 6, span some -30.8 to +44.7 g CO<sub>2e</sub>/MJ-fuel – all of which fall below the RFS2 threshold for all co-product and CPO co-production scenarios. GHG values for the Market CPO case (and Max CPO, though not depicted here) under displacement appear extremely

favorable, moving beyond a carbon neutral process into the regime of carbon negativity. The same can be said of the Market CPO values under market allocation, which still show a substantial reduction over baseline petroleum diesel, albeit not to the extent of displacement. While the variance in GHG values between CPO co-production scenarios is clear, only slight differences evolve between biochar co-product scenarios; the largest of which appears in the Max Fuel case, due to the absence of CPO as a co-product to allocate over.

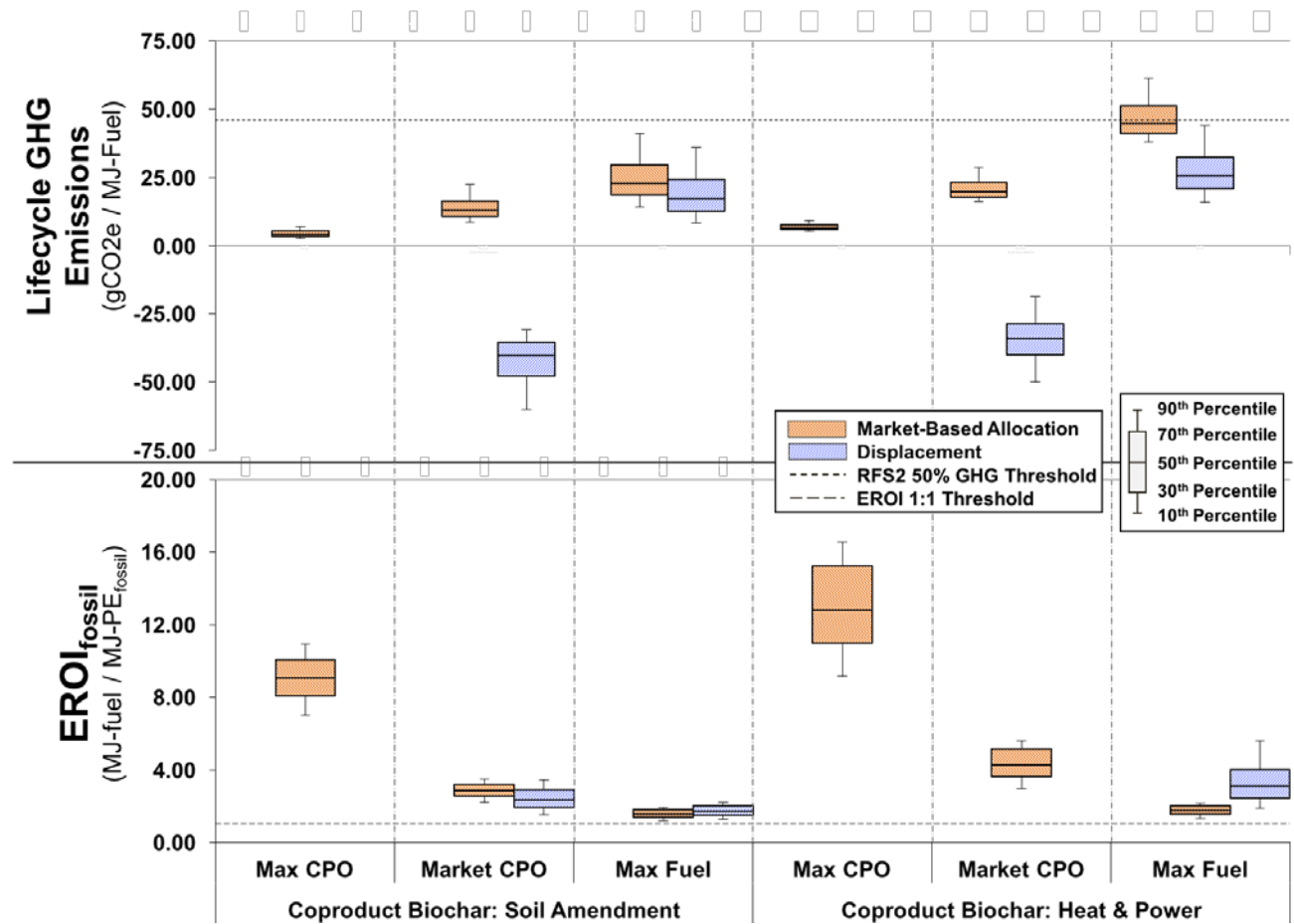


**Figure 12.** Box plots of lifecycle GHG emissions and  $EROI_{fossil}$  percentile values across all co-product scenarios. As per the above legend, boxes' middle line represents median values, and error bars represent the 10<sup>th</sup>-30<sup>th</sup> and 70<sup>th</sup>-90<sup>th</sup> percentile ranges. The RFS2 GHG reduction threshold for diesel is calculated as 50% of 91.94 g CO<sub>2</sub>e /MJ-diesel [5].

In order to provide a higher level of precision in interpreting the above figure, values for the 50th, 10th, and 90th percentiles of lifecycle GHG emissions and  $EROI_{\text{fossil}}$  for all co-production scenarios are also given here in Tables 6 and 7.

**Table 6.** Median values for lifecycle GHG emissions ( $\text{gCO}_2\text{e}/\text{MJ-Fuel}$ ) for all design cases, given in the form X (Y,Z) where X = 50th percentile, Y = 10th percentile, and Z = 90th percentile.

<b>Allocation Scheme</b>	<b>Biochar Co-product Scenario</b>	<b>Max CPO</b>	<b>Market CPO</b>	<b>Max Fuel</b>
<b>Displacement</b>	Soil Amendment	-359 (-371,-333)	-31 (-40,-11)	17 (8,36)
<b>Market Allocation</b>	Soil Amendment	4 (3,7)	13 (8,22)	23 (14,41)
<b>Displacement</b>	Heat & Power	-363 (-376,-338)	-23 (-39,-7)	26 (16,44)
<b>Market Allocation</b>	Heat & Power	6 (5,9)	20 (16,28)	45 (38,61)

**Table 7.** Median values for  $EROI_{\text{fossil}}$  ( $\text{MJ-Fuel}/\text{MJ-Primary Fossil Energy}$ ) for all design cases, given in the form X (Y,Z) where X = 50th percentile, Y = 10th percentile, and Z = 90th percentile.

<b>Allocation Scheme</b>	<b>Biochar Co-product Scenario</b>	<b>Max CPO</b>	<b>Market CPO</b>	<b>Max Fuel</b>
<b>Displacement</b>	Soil Amendment	-1.0 (-1.5,-0.88)	2.4 (1.5,3.4)	1.7 (1.3,2.2)
<b>Market Allocation</b>	Soil Amendment	9.1 (7.0,10.9)	2.9 (2.2,3.5)	1.6 (1.2,1.9)
<b>Displacement</b>	Heat & Power	-0.63 (-0.78,-0.56)	9.7 (4.0,54.6)	3.1 (1.9,5.6)
<b>Market Allocation</b>	Heat & Power	12.8 (9.1,16.6)	4.3 (3.0,5.6)	1.8 (1.3,2.2)

An  $EROI_{\text{fossil}}$  threshold of 1 is often selected to screen for fuels that provide a greater amount of energy (both fossil and/or renewable) than the sum of their lifecycle primary fossil energy inputs

( $PE_{fossil}$ ). Median values for  $EROI_{fossil}$  range from 1.6 to 12.8 MJ-fuel/MJ- $PE_{fossil}$  across all scenarios, and thereby all exceed the minimum desirable threshold value. Looking again at co-product scenarios, combusting biochar for heat and electricity clearly provides consistently higher  $EROI_{fossil}$  values due to the  $PE_{fossil}$  credit from displacing carbon intensive electricity. The same can be said of producing more CPO, but with the caveat of consequently also producing less fuel. Due to the large  $PE_{fossil}$  burden of CPO's standard production from adipic acid, diverting bio-oil away from further upgrading to fuel to instead produce additional CPO tends to increase  $EROI_{fossil}$  drastically via co-product crediting under displacement. Similarly, under market allocation a higher CPO production rate shifts more of the  $PE_{fossil}$  consumption burden away from fuels due to the \$15/kg market price of CPO [37]. Finally, we must note that all Max CPO and one Market CPO values for the displacement method are excluded from Figure 4 due to the enormous GHG and  $PE_{fossil}$  co-product credits for displacing CPO, and the resulting distortions they cause in the LCIA metrics. Under these conditions, these metrics are observed to break down numerically and thereby cease to offer any meaningful interpretation.

As such, displacement is likely unfit to handle co-product allocation for these metrics under the conditions of the aforementioned cases. This assertion is further validated by visualizing the differences between inclusion and exclusion of the contribution of CPO co-product credit for both lifecycle GHG emissions and  $EROI_{\text{fossil}}$  under displacement. Credit for displaced fossil-route CPO is excluded from Figures 13 and 15, and plotted in Figures 14 and 16, alongside arrays of process input burdens and co-product credits with the largest contributions to each respective metric. Individual contributions are taken as average values from the lifecycle inventory and normalized on a per MJ-fuel basis, the functional unit of this study. The summation of all positive and negative contributions are represented as the “WTW GHG Emissions” or “Net Primary Energy Consumption” bars in each plot, provided with error bars spanning the 10<sup>th</sup> to 90<sup>th</sup> percentile values.

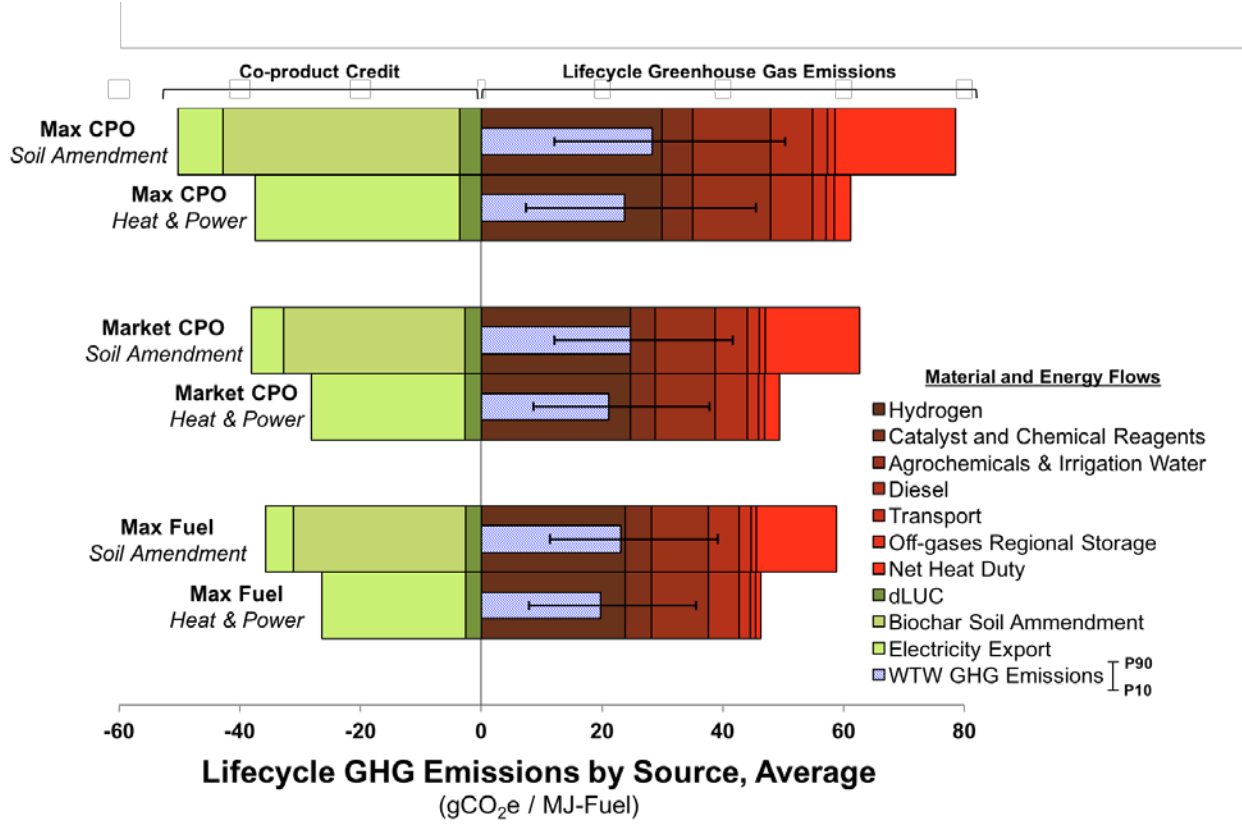


**Figure 13.** Contributions of key process inputs and co-product outputs – including CPO – to lifecycle GHG emissions for all co-production and co-product scenarios under the displacement method.

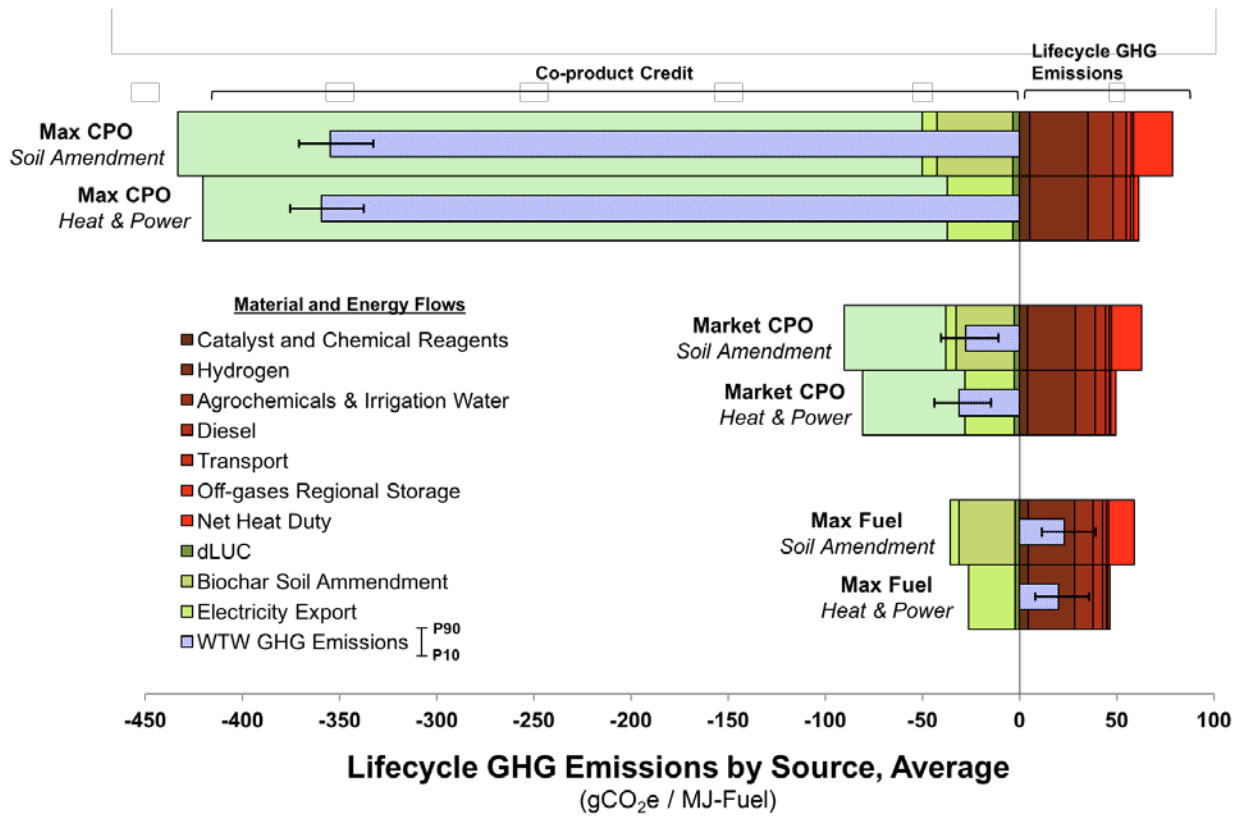


**Figure 14.** Contributions of key process inputs and co-product outputs – including CPO – to lifecycle GHG emissions for all co-production and co-product scenarios under the displacement method.

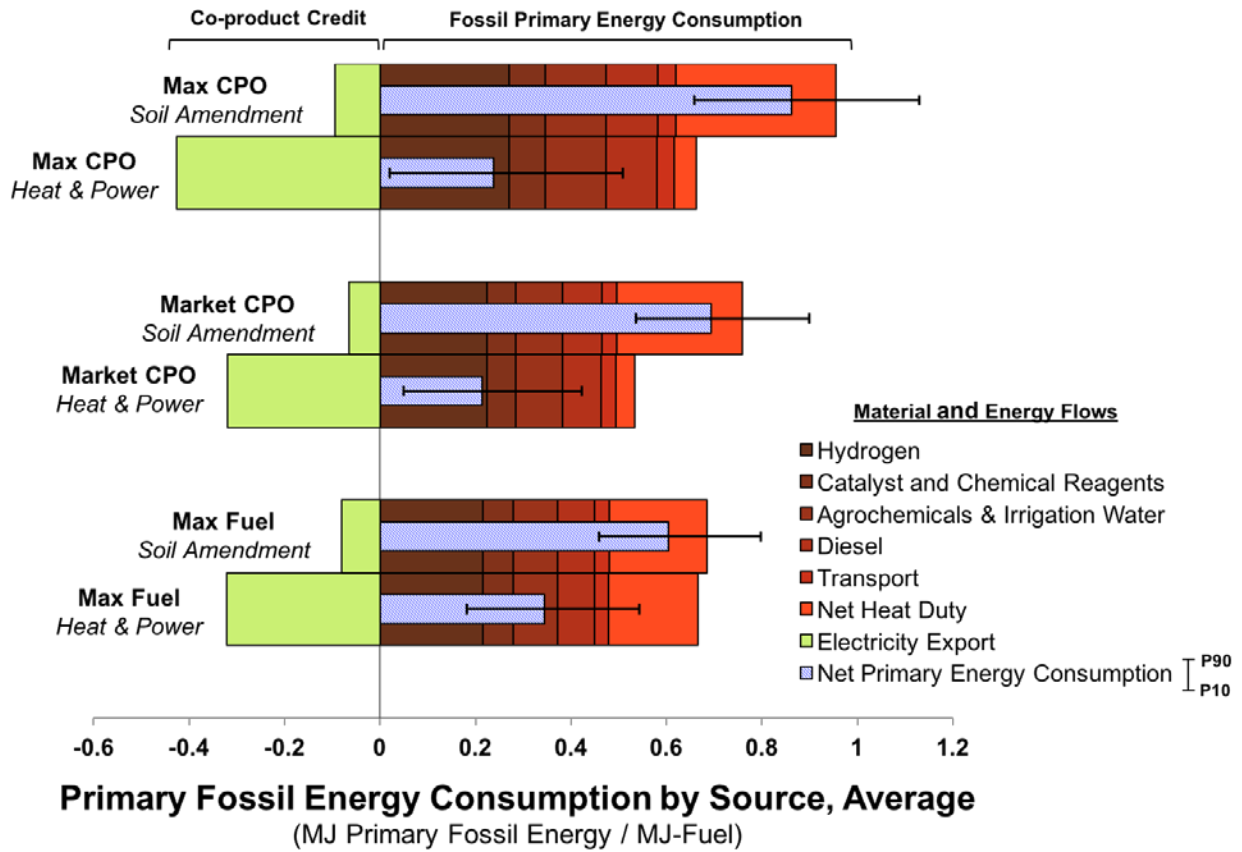


**Figure 15.** Contributions of key process inputs and co-product outputs – excluding CPO – to lifecycle primary fossil energy consumption for all co-production and co-product scenarios under the displacement method.

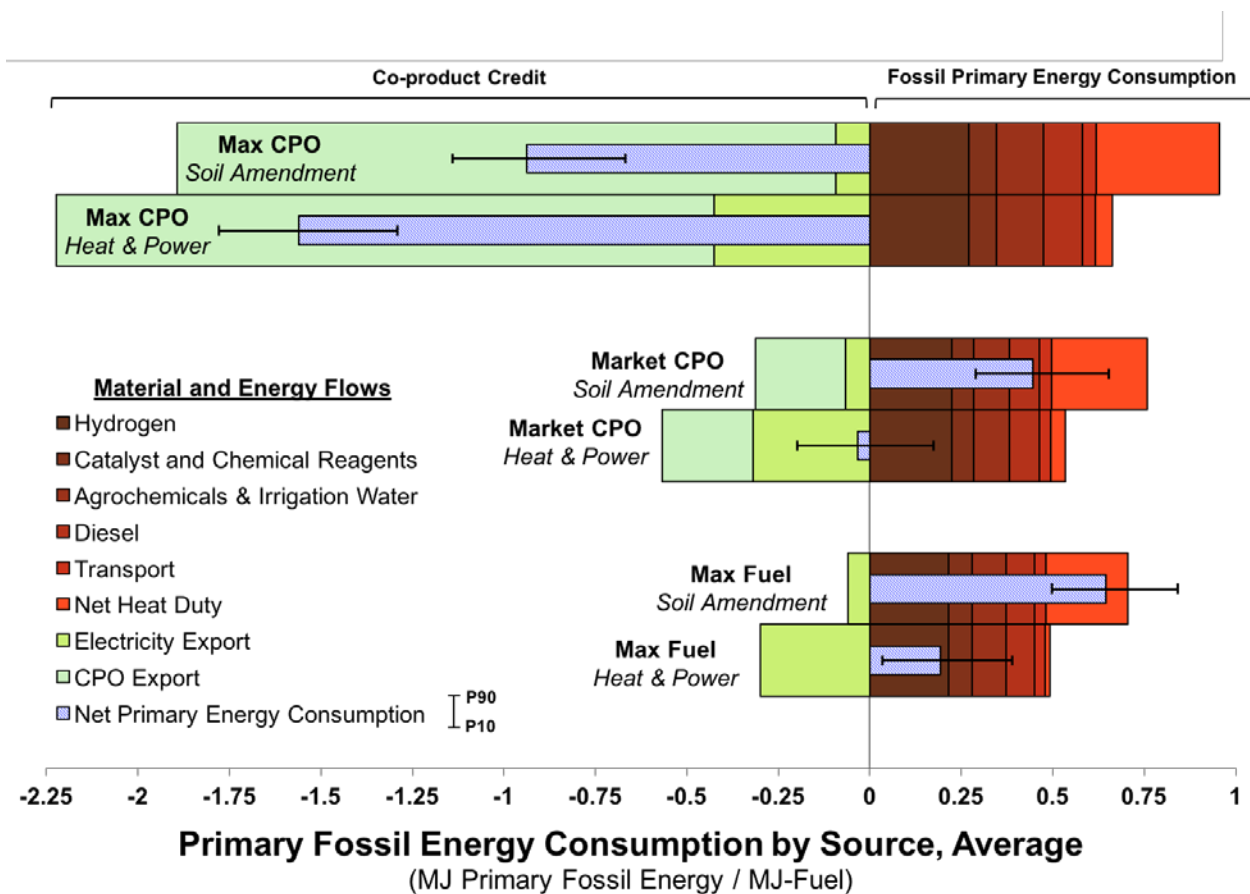


**Figure 16.** Contributions of key process inputs and co-product outputs – including CPO – to lifecycle primary fossil energy consumption for all co-production and co-product scenarios under the displacement method.

While excluding CPO in Figures 13 and 15, both the Net Heat Duty, Agrochemicals & Irrigation Water, and process Hydrogen consumption all consistently contribute the most to lifecycle GHG emissions and fossil primary energy consumption. Net heating duty in particular varies strongly across biochar co-product scenarios due to the generation of process heat in the CHP case and the carbon intensity of generating the remainder of the heat by combusting natural gas in a boiler. The primary contributor to the Agrochemicals & Irrigation Water category for both primary energy and GHGs is synthetic nitrogen fertilizers, due to the large natural gas and electricity requirements inherent in their production. It should be noted that the biochar soil

amendment, direct land use change (dLUC), and off-gases from regional storage categories only appear in the lifecycle GHG emissions plots, since their constituent activities are defined so as not to involve the consumption of energy products. Additionally, due to the Max CPO case producing less fuel than the Market CPO case, which produces less than the Max Fuel case, each of the positive and negative contributions for the CPO-producing cases are marginally increased in comparison to the Max Fuel case.

Looking again at lifecycle GHG emissions in Figure 13, the difference between the co-product credit for just electricity exports under the Heat & Power scenario vs. the total of both electricity exports and biochar soil amendment under the Soil Amendment scenario appears substantial, but upon inclusion of CPO co-product credit, the difference quickly becomes irrelevant. For both GHG and primary energy consumption, the negative credits for CPO production immensely outweigh the remainder of the contributions over the lifecycle, due to the high fossil energy intensity of producing CPO via the adipic acid route. Such immense co-product credits are indeed unrealistic for the Max CPO case, since the Market CPO case was itself formulated to produce an amount equivalent to a global demand projected for 2020. Additionally, attributional LCA may not fully capture the secondary and higher-order effects of flooding the marketplace with CPO, and the alternative approach of consequential LCA is discussed further in the Conclusions section.

## 4.5 SENSITIVITY ANALYSIS

Within the Market CPO case, eight model parameters – liquid fuel yield, H<sub>2</sub> consumption, biochar yield, SRWC growth rate, urea application rate, CPO yield, fuel price, and CPO price – were varied by  $\pm 20\%$  to determine their relative levels of influence on the median values of LCIA metrics, and how those effects changed under the various co-product scenarios and allocation methods. Tornado plots for both lifecycle GHG emissions and  $EROI_{\text{fossil}}$  under market-based allocation are shown in Figure 17, and results under displacement are given subsequently in Figure 18. The  $EROI_{\text{fossil}}$ , Heat & Power scenario of the latter figure experiences a numerical distortion derived from the limitations of how the  $EROI_{\text{fossil}}$  metric is formulated, wherein reducing the biochar yield results in a shift in the metric's denominator from a negative value to a positive value. This asymptotic limitation built into the co-product crediting method is discussed in further detail in the Conclusions section. Finally, neither fuel price nor CPO price affect the LCIA metrics in Figure 18, as would be expected for the displacement method.

In stark contrast to the models investigated in Zaines et. al 2017, the systems investigated here show little to no dependence on liquid fuel yield, but instead show a consistent, large dependence on CPO yield. At a similar level of influence, H<sub>2</sub> consumption consistently affects GHG emissions and  $PE_{\text{fossil}}$ , due to the fossil energy intensity of H<sub>2</sub> production via steam-methane reforming. With this strong dependence in mind during the design process, C-C coupling reactions were extensively employed to increase liquid fuel yield while simultaneously decreasing process H<sub>2</sub> requirements. Using biochar as a soil amendment, biochar yield has the largest influence over lifecycle GHG emissions, while simultaneously having almost no effect on

EROI<sub>fossil</sub>. Finally, to better understand market allocation in particular, both CPO price and fuel price are investigated, both proving to be strong determinants of both lifecycle GHG emissions and EROI metrics under all scenarios.

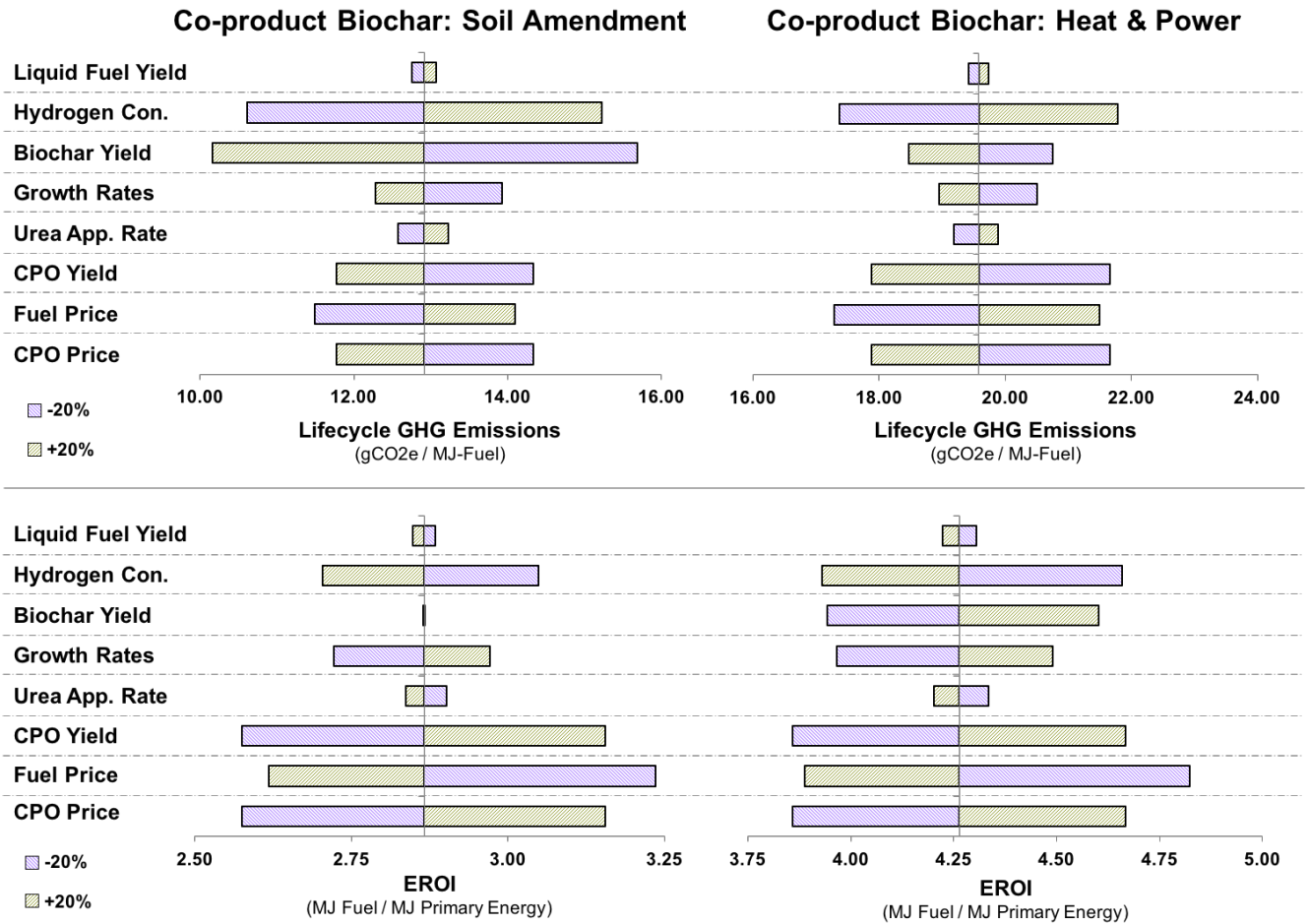


**Figure 17.** Sensitivity results for 8 model parameters for the Market CPO production case, evaluated under market allocation by varying parameters  $\pm 20\%$ .

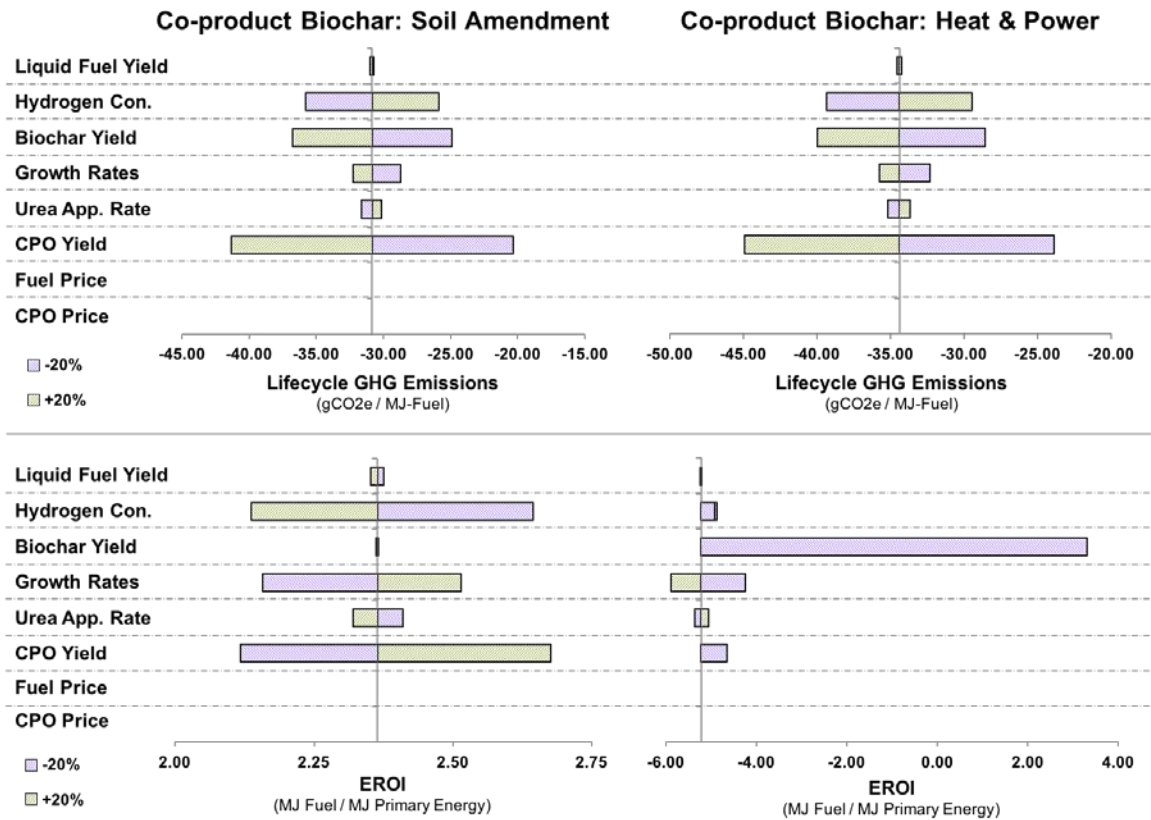


**Figure 18.** Sensitivity results for 8 model parameters for the Market CPO production case, evaluated under displacement by varying parameters  $\pm 20\%$ . Fuel Price and CPO price do not affect the LCIA metrics, as would be expected for displacement. Reducing Biochar Yield's affects  $EROI_{fossil}$  in such a way as to shift the metric's denominator from a negative value to a positive value, producing the distorted result shown here.

## 5.0 CONCLUSIONS AND FUTURE WORK

### 5.1 METHODOLOGICAL LIMITATIONS

Leaving aside the ongoing net-energy analysis issues of aggregating energy sources of different entropic quality [64] and CED including energy flows not seen by society [65], the present work arrives at problems of primary product selection for system boundary expansion [66] and of co-product crediting within the formulation of EROI metrics. As first formalized by Wang et al. 2011 and repeatedly identified by others [23, 67], where non-fuel products become a substantial share of the mass, energy or revenue output of a process, the displacement method may no longer produce reasonable results for the primary fuel product [66]. While Table 8 shows CPO to consistently be a small share of the total mass output (0-31%) relative to the primary biofuel product, CPO's share of 71% of the total revenue output in the Market CPO case is the condition under which displacement ceases to provide meaningful results.

**Table 8.** Primary product (biofuel) and co-product shares of total mass and revenue outputs

<b>Product Shares of Total Output</b>	<b>Max CPO</b>		<b>Market CPO</b>		<b>Max Fuel</b>	
	<i>Mass</i>	<i>Revenue</i>	<i>Mass</i>	<i>Revenue</i>	<i>Mass</i>	<i>Revenue</i>
<b>Biofuel (C6+)</b>	69%	27%	94%	71%	100%	96%
<b>Cyclopentanone</b>	31%	71%	6%	26%	0%	0%
<b>Electricity</b>	-	1%	-	3%	-	4%

One potential option for addressing this may simply be swapping CPO for biofuel as the primary product in the Max CPO case. Performing a consequential LCA could also serve to alleviate this issue, which partially hinges on the price inelasticity built into the attributional LCA model. While a shift from attributional to consequential LCA could possibly remedy the issue of extreme negative lifecycle GHG emissions values for the Max CPO case, it may fall short in addressing how co-product credit applies to EROI metrics. As the total co-product credit approaches the value of the total  $PE_{\text{fossil}}$ , the denominator of  $EROI_{\text{fossil}}$  approaches 0, and pushes the metric toward infinity, followed by sending it into the negative regime. While a consequential LCA could hinder the co-product's market substitutability and total credit accrued, it still cannot guarantee avoidance of this latter problem for primary products of low CED and co-products of substantial CED. As such, system boundary expansion in the context of EROI will likely require more robust mathematical formulations than simply subtracting values from a denominator. Without a mathematical standard that addresses this, the adjacent issue of different studies arriving at different EROI values due to selecting different allocation methods [68, 69] may also continue, unabated.

Further affecting the comparability of LCA studies, selection of functional unit, system boundary, allocation schemes, and lifecycle metrics are explicitly, repeatedly stated in this study, due to their substantial influence on the results presented here. Rigid selection of differing allocation scheme(s) and end-use scenario(s) for just biochar has complicated the comparability of multiple studies [70, 71], let alone additional co-products. In tandem, certain authors argue that the ISO standard of strictly preferring system boundary expansion over allocation is too rigid [11], and the distortions produced under the circumstances of this work stand as another data point to oppose said standard. This is all to say, without explicit acknowledgement of these study

design parameters, LCAs of biofuels are effectively incomparable and cannot contribute to the larger research community [72]. Beyond these communicable details, spatiotemporal variation in land-uses, resource use, climatic conditions, adjacent ecosystems systems, and points of emissions release all affect results of LCA studies – and especially agriculture-based biofuel studies – as well [73-75]. These sources of variance are unavoidable without highly region-specific modelling work, and are still an area of active research and debate amongst LCA practitioners [76]. Adding one final layer to these challenges, issues of data quality, data averaging, and reliance on point estimates all generally tend to invalidate traditional attributional LCA studies, necessitating statistical approaches such as Monte Carlo simulations and one-factor-at-a-time sensitivity methods, among others [77]. Attention to set of these considerations, and their interactions, is no longer optional if we are to construct comparable, realistic LCA models for emerging technologies.

## 5.2 FUTURE WORK

While the present work focuses only on lifecycle GHG emissions and  $EROI_{\text{fossil}}$ , a host of other lifecycle metrics such as lifecycle water footprint and production of air, water, and solid waste pollutants could be explored so as to lend further comparability between the produced bio-based fuels and chemicals versus fossil fuels and petrochemicals, avoid unintended consequences [78-80], and explore lifecycle trade-offs [81, 82]. The economic feasibility of this work and similar systems should also be addressed, in the form of techno-economic assessment studies with a focus on bio-based fuel and chemical co-production strategies. Despite market sizes for specialty chemicals producible from biomass being smaller than that of fuel markets, co-producing fuels and

chemicals could still provide a pathway for commercialization of biorefineries, and deserves further attention in general. Finally, economic viability cannot be accurately assessed under low-carbon fuel incentives without rigorous, systemic lifecycle environmental studies involving scenario, uncertainty, and sensitivity analyses; nor can the effective enforcement and potency of low-carbon fuel incentives be guaranteed without these elements.

## BIBLIOGRAPHY

- [1] R. K. Pachauri, M. R. Allen, V. R. Barros, J. Broome, W. Cramer, R. Christ, *et al.*, "Climate Change 2014: Synthesis Report. Contribution of Working Groups I, II and III to the Fifth Assessment Report of the Intergovernmental Panel on Climate Change," 2014.
- [2] R. S. Sims R., F. Creutzig, X. Cruz-Núñez, M. D'Agosto, D. Dimitriu, M. J. Figueroa Meza, L. Fulton, S. Kobayashi, O. Lah, A. McKinnon, P. Newman, M. Ouyang, J. J. Schauer, D. Sperling, G. Tiwari, "2014: Transport. In: Climate Change 2014: Mitigation of Climate Change. Contribution of Working Group III to the Fifth Assessment Report of the Intergovernmental Panel on Climate Change," 2014.
- [3] EPA, "Inventory of U.S. Greenhouse Gas Emissions and Sinks: 1990 - 2015," ed: US Environmental Protection Agency Washington, DC, 2017, p. 663.
- [4] M. Balat and H. Balat, "Recent trends in global production and utilization of bio-ethanol fuel," *Applied Energy*, vol. 86, pp. 2273-2282, 2009/11/01/ 2009.
- [5] EPA, "Regulation of Fuels and Fuel Additives: Changes to Renewable Fuel Standard Program; Final Rule (2010)," vol. EPA-HQ-OAR-2005-01612010, pp. 14669-15320, 2010.
- [6] D. Andress, T. Dean Nguyen, and S. Das, "Low-carbon fuel standard—Status and analytic issues," *Energy Policy*, vol. 38, pp. 580-591, 2010/01/01/ 2010.
- [7] F. Sissine, "Energy Independence and Security Act of 2007: A Summary of Major Provisions," Congressional Research Service Report for Congress, Order Code RL34294, Washington, DC2007.
- [8] J. E. Oliver, "Kyoto Protocol," in *Encyclopedia of World Climatology*, J. E. Oliver, Ed., ed Dordrecht: Springer Netherlands, 2005, pp. 443-443.
- [9] "Paris Agreement," ed. United Nations Treaty Collection: United Nations Framework Convention on Climate Change, 2015, p. 7.
- [10] European Parliament & Council, "EC (2009) Directive 2009/28/EC of the European Parliament and of the Council of 23 April 2009 on the promotion of the use of energy from renewable sources and amending and subsequently repealing Directives 2001/77/EC and 2003/30/EC.," 2009.

- [11] A. S. Kaufman, P. J. Meier, J. C. Sinistore, and D. J. Reinemann, "Applying life-cycle assessment to low carbon fuel standards—How allocation choices influence carbon intensity for renewable transportation fuels," *Energy Policy*, vol. 38, pp. 5229-5241, 2010/09/01/ 2010.
- [12] S. Nonhebel, "Global food supply and the impacts of increased use of biofuels," *Energy*, vol. 37, pp. 115-121, 2012/01/01/ 2012.
- [13] D. Pimentel, T. Patzek, and G. Cecil, "Ethanol Production: Energy, Economic, and Environmental Losses," in *Reviews of Environmental Contamination and Toxicology: Continuation of Residue Reviews*, D. M. Whitacre, G. W. Ware, H. N. Nigg, D. R. Doerge, L. A. Albert, P. de Voogt, *et al.*, Eds., ed New York, NY: Springer New York, 2007, pp. 25-41.
- [14] R. Hammerschlag, "Ethanol's Energy Return on Investment: A Survey of the Literature 1990–Present," *Environmental Science & Technology*, vol. 40, pp. 1744-1750, 2006/03/01 2006.
- [15] R. Sims, M. Taylor, J. Saddler, and W. Mabee, "From 1st-to 2nd-Generation Biofuel Technologies: An overview of current industry and RD&D activities," *International Energy Agency and Organization for Economic Cooperation and Development*, 2008.
- [16] T. Searchinger, R. Heimlich, R. A. Houghton, F. X. Dong, A. Elobeid, J. Fabiosa, *et al.*, "Use of US croplands for biofuels increases greenhouse gases through emissions from land-use change," *Science*, vol. 319, pp. 1238-1240, Feb 29 2008.
- [17] J. Fargione, J. Hill, D. Tilman, S. Polasky, and P. Hawthorne, "Land Clearing and the Biofuel Carbon Debt," *Science*, vol. 319, pp. 1235-1238, 2008.
- [18] J. Rockstrom, W. Steffen, K. Noone, A. Persson, F. S. Chapin, E. F. Lambin, *et al.*, "A safe operating space for humanity," *Nature*, vol. 461, pp. 472-475, 09/24/print 2009.
- [19] W. Steffen, K. Richardson, J. Rockström, S. E. Cornell, I. Fetzer, E. M. Bennett, *et al.*, "Planetary boundaries: Guiding human development on a changing planet," *Science*, vol. 347, 2015.
- [20] S. B. Jones, C. Valkenburg, C. W. Walton, D. C. Elliott, J. E. Holladay, D. J. Stevens, *et al.*, "Production of gasoline and diesel from biomass via fast pyrolysis, hydrotreating and hydrocracking: a design case," Pacific Northwest National Laboratory Richland, WA2009. [http://www.pnl.gov/main/publications/external/technical\\_reports/pnnl-18284.pdf](http://www.pnl.gov/main/publications/external/technical_reports/pnnl-18284.pdf).
- [21] M. M. Wright, D. E. Dugaard, J. A. Satrio, and R. C. Brown, "Techno-economic analysis of biomass fast pyrolysis to transportation fuels," *Fuel*, vol. 89, Supplement 1, pp. S2-S10, 11/1/ 2010.

- [22] Y. Zhang, G. Hu, and R. C. Brown, "Life cycle assessment of the production of hydrogen and transportation fuels from corn stover via fast pyrolysis," *Environmental Research Letters*, vol. 8, p. 025001, 2013.
- [23] G. G. Zaimes, K. Soratana, C. L. Harden, A. E. Landis, and V. Khanna, "Biofuels via Fast Pyrolysis of Perennial Grasses: A Life Cycle Evaluation of Energy Consumption and Greenhouse Gas Emissions," *Environmental Science & Technology*, vol. 49, pp. 10007-10018, 2015/08/18 2015.
- [24] K. Wang and R. C. Brown, "Catalytic Pyrolysis of Corn Dried Distillers Grains with Solubles to Produce Hydrocarbons," *ACS Sustainable Chemistry & Engineering*, vol. 2, pp. 2142-2148, 2014/09/02 2014.
- [25] K. G. Roberts, B. A. Gloy, S. Joseph, N. R. Scott, and J. Lehmann, "Life Cycle Assessment of Biochar Systems: Estimating the Energetic, Economic, and Climate Change Potential," *Environmental Science & Technology*, vol. 44, pp. 827-833, 2010/01/15 2010.
- [26] L. Van Zwieten, S. Kimber, S. Morris, K. Y. Chan, A. Downie, J. Rust, *et al.*, "Effects of biochar from slow pyrolysis of papermill waste on agronomic performance and soil fertility," *Plant and Soil*, vol. 327, pp. 235-246, February 01 2010.
- [27] S. Shabangu, D. Woolf, E. M. Fisher, L. T. Angenent, and J. Lehmann, "Techno-economic assessment of biomass slow pyrolysis into different biochar and methanol concepts," *Fuel*, vol. 117, pp. 742-748, 2014/01/30/ 2014.
- [28] B. Strogen, A. Horvath, and T. E. McKone, "Fuel Miles and the Blend Wall: Costs and Emissions from Ethanol Distribution in the United States," *Environmental Science & Technology*, vol. 46, pp. 5285-5293, 2012/05/15 2012.
- [29] S. Ukaew, R. Shi, J. H. Lee, D. W. Archer, M. Pearlson, K. C. Lewis, *et al.*, "Full Chain Life Cycle Assessment of Greenhouse Gases and Energy Demand for Canola-Derived Jet Fuel in North Dakota, United States," *ACS Sustainable Chemistry & Engineering*, vol. 4, pp. 2771-2779, 2016/05/02 2016.
- [30] J. A. Herron, T. Vann, N. Duong, D. E. Resasco, S. Crossley, L. L. Lobban, *et al.*, "A Systems-Level Roadmap for Biomass Thermal Fractionation and Catalytic Upgrading Strategies," *Energy Technology*, pp. n/a-n/a, 2016.
- [31] G. G. Zaimes, A. W. Beck, R. R. Janupala, D. E. Resasco, S. P. Crossley, L. L. Lobban, *et al.*, "Multistage torrefaction and in situ catalytic upgrading to hydrocarbon biofuels: analysis of life cycle energy use and greenhouse gas emissions," *Energy & Environmental Science*, vol. 10, pp. 1034-1050, 2017.
- [32] O. Winjobi, W. Zhou, D. Kulas, J. Nowicki, and D. R. Shonnard, "Production of Hydrocarbon Fuel Using Two-Step Torrefaction and Fast Pyrolysis of Pine. Part 2: Life-Cycle Carbon Footprint," *ACS Sustainable Chemistry & Engineering*, vol. 5, pp. 4541-4551, 2017/06/05 2017.

- [33] V. Balan, "Current Challenges in Commercially Producing Biofuels from Lignocellulosic Biomass," *ISRN Biotechnology*, vol. 2014, p. 31, 2014.
- [34] W. Hu, Q. Dang, M. Rover, R. C. Brown, and M. M. Wright, "Comparative techno-economic analysis of advanced biofuels, biochemicals, and hydrocarbon chemicals via the fast pyrolysis platform," *Biofuels*, vol. 7, pp. 57-67, 2016/01/02 2016.
- [35] Q. Dang, W. Hu, M. Rover, R. C. Brown, and M. M. Wright, "Economics of biofuels and bioproducts from an integrated pyrolysis biorefinery," *Biofuels, Bioproducts and Biorefining*, vol. 10, pp. 790-803, 2016.
- [36] M. J. S. Bidy, C.; Kinchin, C., "Chemicals from Biomass: A Market Assessment of Bioproducts with Near-Term Potential," National Renewable Energy Laboratory March 2016 2016.
- [37] "Cyclopentanone Market for Pharmaceuticals, Biological, Perfumes & Aromas, Rubber Chemicals, Insecticides and Other Applications: Global Industry Perspective, Comprehensive Analysis, Size, Share, Growth, Segment, Trends and Forecast, 2014 – 2020," Zion Market Research 2016.
- [38] J. Guo, G. Xu, Z. Han, Y. Zhang, Y. Fu, and Q. Guo, "Selective Conversion of Furfural to Cyclopentanone with CuZnAl Catalysts," *ACS Sustainable Chemistry & Engineering*, vol. 2, pp. 2259-2266, 2014/10/06 2014.
- [39] G. G. Zaimes, A. W. Beck, R. J. Reddy, D. Resasco, S. Crossley, I. Iobban, *et al.*, "Multistage torrefaction and in situ catalytic upgrading to hydrocarbon biofuels: analysis of life cycle energy use and greenhouse gas emissions," *Energy & Environmental Science*, 2017.
- [40] M. Hronec, K. Fulajtarová, and T. Liptaj, "Effect of catalyst and solvent on the furan ring rearrangement to cyclopentanone," *Applied Catalysis A: General*, vol. 437, pp. 104-111, 2012/09/26/ 2012.
- [41] Y. E. Sorunmu, P. Billen, Y. Elkasabi, C. A. Mullen, N. A. Macken, A. A. Boateng, *et al.*, "Fuels and Chemicals from Equine-Waste-Derived Tail Gas Reactive Pyrolysis Oil: Technoeconomic Analysis, Environmental and Exergetic Life Cycle Assessment," *ACS Sustainable Chemistry & Engineering*, vol. 5, pp. 8804-8814, 2017/10/02 2017.
- [42] S. Kim and J. Han, "Enhancement of energy efficiency and economics of process designs for catalytic co-production of bioenergy and bio-based products from lignocellulosic biomass," *International Journal of Energy Research*, vol. 41, pp. 1553-1562, 2017.
- [43] International Organization for Standardization, "ISO 14040 Environmental management - Life cycle assessment - Principles and framework," ed. Switzerland, 2006.
- [44] B. A. Wender, R. W. Foley, T. A. Hottle, J. Sadowski, V. Prado-Lopez, D. A. Eisenberg, *et al.*, "Anticipatory life-cycle assessment for responsible research and innovation," *Journal of Responsible Innovation*, vol. 1, pp. 200-207, 2014/05/04 2014.

- [45] E. Ahmetović, M. Martín, and I. E. Grossmann, "Optimization of Energy and Water Consumption in Corn-Based Ethanol Plants," *Industrial & Engineering Chemistry Research*, vol. 49, pp. 7972-7982, 2010/09/01 2010.
- [46] G. J. Ruiz-Mercado, A. Carvalho, and H. Cabezas, "Using Green Chemistry and Engineering Principles To Design, Assess, and Retrofit Chemical Processes for Sustainability," *ACS Sustainable Chemistry & Engineering*, vol. 4, pp. 6208-6221, 2016/11/07 2016.
- [47] K. G. Roberts, B. A. Gloy, S. Joseph, N. R. Scott, and J. Lehmann, "Life Cycle Assessment of Biochar Systems: Estimating the Energetic, Economic, and Climate Change Potential," *Environmental Science & Technology*, vol. 44, pp. 827-833, 2010/01/15 2009.
- [48] C. E. Canter, J. B. Dunn, J. Han, Z. Wang, and M. Wang, "Policy Implications of Allocation Methods in the Life Cycle Analysis of Integrated Corn and Corn Stover Ethanol Production," *BioEnergy Research*, vol. 9, pp. 77-87, March 01 2016.
- [49] A. Corma, O. de la Torre, and M. Renz, "Production of high quality diesel from cellulose and hemicellulose by the Sylvan process: catalysts and process variables," *Energy & Environmental Science*, vol. 5, pp. 6328-6344, 2012.
- [50] Q. Deng, P. Han, J. Xu, J.-J. Zou, L. Wang, and X. Zhang, "Highly controllable and selective hydroxyalkylation/alkylation of 2-methylfuran with cyclohexanone for synthesis of high-density biofuel," *Chemical Engineering Science*, vol. 138, pp. 239-243, 12/22/ 2015.
- [51] J. Donnelly, R. Horton, K. Gopalan, C. D. Bannister, and C. J. Chuck, "Branched Ketone Biofuels as Blending Agents for Jet-A1 Aviation Kerosene," *Energy & Fuels*, vol. 30, pp. 294-301, 2016/01/21 2016.
- [52] D. Santhanaraj, M. R. Rover, D. E. Resasco, R. C. Brown, and S. Crossley, "Gluconic acid from biomass fast pyrolysis oils: specialty chemicals from the thermochemical conversion of biomass," *ChemSusChem*, vol. 7, pp. 3132-3137, 2014.
- [53] T. V. Bui, T. Sooknoi, and D. E. Resasco, "Simultaneous Upgrading of Furanics and Phenolics through Hydroxyalkylation/Aldol Condensation Reactions," *ChemSusChem*, vol. 10, pp. 1631-1639, 2017.
- [54] Z. Miao, T. E. Grift, A. C. Hansen, and K. C. Ting, "Energy requirement for comminution of biomass in relation to particle physical properties," *Industrial Crops and Products*, vol. 33, pp. 504-513, 3// 2011.
- [55] A. Roedl, "Production and energetic utilization of wood from short rotation coppice—a life cycle assessment," *The International Journal of Life Cycle Assessment*, vol. 15, pp. 567-578, 2010// 2010.

- [56] D. Dressler, A. Loewen, and M. Nelles, "Life cycle assessment of the supply and use of bioenergy: impact of regional factors on biogas production," *The International Journal of Life Cycle Assessment*, vol. 17, pp. 1104-1115, 2012// 2012.
- [57] P. T. Benavides, D. C. Cronauer, F. Adom, Z. Wang, and J. B. Dunn, "The influence of catalysts on biofuel life cycle analysis (LCA)," *Sustainable Materials and Technologies*, vol. 11, pp. 53-59, 4// 2017.
- [58] S. B. Jones, L. J. Snowden-Swan, P. A. Meyer, A. H. Zacher, M. V. Olarte, and C. Drennan, "Fast Pyrolysis and Hydrotreating: 2013 State of Technology R&D and Projections to 2017," Pacific Northwest National Laboratory (PNNL), Richland, WA (US)2014.
- [59] T. F. Stocker, D. Qin, G. K. Plattner, M. Tignor, S. K. Allen, J. Boschung, *et al.*, "IPCC, 2013: climate change 2013: the physical science basis. Contribution of working group I to the fifth assessment report of the intergovernmental panel on climate change," 2013.
- [60] Cumulative Energy Demand, "Terms, definitions, methods of calculation," *Association of German Engineers*, 1997.
- [61] G. Wernet, C. Bauer, B. Steubing, J. Reinhard, E. Moreno-Ruiz, and B. Weidema, "The ecoinvent database version 3 (part I): overview and methodology," *The International Journal of Life Cycle Assessment*, vol. 21, pp. 1218-1230, September 01 2016.
- [62] "Petroleum & Other Liquids: U.S. No 2 Diesel Ultra Low Sulfur (0-15ppm) Retail prices," ed. U.S. Energy Information Administration, 2017.
- [63] "Average Price of Electricity to Ultimate Customers: Total by End-Use Sector, 2007 - August 2017 (Cents per Kilowatthour)," ed. U.S. Energy Information Administration, 2017.
- [64] D. J. Murphy, C. A. S. Hall, M. Dale, and C. Cleveland, "Order from Chaos: A Preliminary Protocol for Determining the EROI of Fuels," *Sustainability*, vol. 3, p. 1888, 2011.
- [65] A. Arvesen and E. G. Hertwich, "More caution is needed when using life cycle assessment to determine energy return on investment (EROI)," *Energy Policy*, vol. 76, pp. 1-6, 2015/01/01/ 2015.
- [66] M. Wang, H. Huo, and S. Arora, "Methods of dealing with co-products of biofuels in life-cycle analysis and consequent results within the U.S. context," *Energy Policy*, vol. 39, pp. 5726-5736, 10// 2011.
- [67] G. G. Zaines and V. Khanna, "The role of allocation and coproducts in environmental evaluation of microalgal biofuels: How important?," *Sustainable Energy Technologies and Assessments*, vol. 7, pp. 247-256, 9// 2014.
- [68] C. A. S. Hall, B. E. Dale, and D. Pimentel, "Seeking to Understand the Reasons for Different Energy Return on Investment (EROI) Estimates for Biofuels," *Sustainability*, vol. 3, p. 2413, 2011.

- [69] M. Montazeri, G. G. Zaimes, V. Khanna, and M. J. Eckelman, "Meta-Analysis of Life Cycle Energy and Greenhouse Gas Emissions for Priority Biobased Chemicals," *ACS Sustainable Chemistry & Engineering*, vol. 4, pp. 6443-6454, 2016/12/05 2016.
- [70] M. J. C. Van der Stelt, H. Gerhauser, J. H. A. Kiel, and K. J. Ptasinski, "Biomass upgrading by torrefaction for the production of biofuels: A review," *Biomass and bioenergy*, vol. 35, pp. 3748-3762, 2011.
- [71] J. Han, A. Elgowainy, J. B. Dunn, and M. Q. Wang, "Life cycle analysis of fuel production from fast pyrolysis of biomass," *Bioresource Technology*, vol. 133, pp. 421-428, 2013/04/01/ 2013.
- [72] G. G. Zaimes and V. Khanna, "Chapter 8 - Life cycle sustainability aspects of microalgal biofuels," in *Assessing and Measuring Environmental Impact and Sustainability*, J. J. Klemeš, Ed., ed Oxford: Butterworth-Heinemann, 2015, pp. 255-276.
- [73] A. Mosnier, P. Havlík, H. Valin, J. Baker, B. Murray, S. Feng, *et al.*, "Alternative U.S. biofuel mandates and global GHG emissions: The role of land use change, crop management and yield growth," *Energy Policy*, vol. 57, pp. 602-614, 2013/06/01/ 2013.
- [74] A. Kendall and J. Yuan, "Comparing life cycle assessments of different biofuel options," *Current Opinion in Chemical Biology*, vol. 17, pp. 439-443, 2013/06/01/ 2013.
- [75] E. Gawel and G. Ludwig, "The iLUC dilemma: How to deal with indirect land use changes when governing energy crops?," *Land Use Policy*, vol. 28, pp. 846-856, 2011/10/01/ 2011.
- [76] A. Broch, S. K. Hoekman, and S. Unnasch, "A review of variability in indirect land use change assessment and modeling in biofuel policy," *Environmental Science & Policy*, vol. 29, pp. 147-157, 2013/05/01/ 2013.
- [77] T. E. McKone, W. W. Nazaroff, P. Berck, M. Auffhammer, T. Lipman, M. S. Torn, *et al.*, "Grand challenges for life-cycle assessment of biofuels," *Environmental science & technology*, vol. 45, pp. 1751-1756, 2011/03/01 2011.
- [78] D. A. Landis, M. M. Gardiner, W. van der Werf, and S. M. Swinton, "Increasing corn for biofuel production reduces biocontrol services in agricultural landscapes," *Proceedings of the National Academy of Sciences*, vol. 105, pp. 20552-20557, December 23, 2008 2008.
- [79] K. Soratana, V. Khanna, and A. E. Landis, "Re-envisioning the renewable fuel standard to minimize unintended consequences: A comparison of microalgal diesel with other biodiesels," *Applied Energy*, vol. 112, pp. 194-204, 12// 2013.
- [80] A. Gasparatos, P. Stromberg, and K. Takeuchi, "Biofuels, ecosystem services and human wellbeing: Putting biofuels in the ecosystem services narrative," *Agriculture, Ecosystems & Environment*, vol. 142, pp. 111-128, 2011/08/01/ 2011.

- [81] L. Čuček, J. J. Klemeš, and Z. Kravanja, "Carbon and nitrogen trade-offs in biomass energy production," *Clean Technologies and Environmental Policy*, vol. 14, pp. 389-397, June 01 2012.
- [82] G. G. Zaines, N. Vora, S. S. Chopra, A. E. Landis, and V. Khanna, "Design of Sustainable Biofuel Processes and Supply Chains: Challenges and Opportunities," *Processes*, vol. 3, pp. 634-663, 2015.